buildings

MDPI

Article

Applying the Dragonfly Algorithm in Reducing Site Risks in Construction Site Layout Planning

Yilmaz Ogunc Tetik [1,*] and Selim Baradan [2]

[1] School of Engineering, Newcastle University, Newcastle upon Tyne NE1 7RU, UK
[2] Department of Civil Engineering, Ege University, Izmir 35040, Turkey; selim.baradan@ege.edu.tr
* Correspondence: yilmaz.tetik@newcastle.ac.uk

Abstract

Construction site layout planning (CSLP) is an optimization issue that has been studied for decades. However, risk factors are still open to exploration, and risk is often not addressed comprehensively in the state-of-the-art literature; moreover, only a few studies have investigated safety as an optimization component in construction sites. This research aims to obtain optimal layout solutions that minimize site risk. In this study, the components of the risk factor were defined as interaction flows between facilities, closeness factors, and the influence of tower cranes. The Dragonfly Algorithm (DA) was selected to solve the CSLP problem due to its strong exploration and exploitation capacity. A DA-based model was developed that integrates the relationships between facilities into a single objective function. This integration extends existing CSLP optimization frameworks by explicitly incorporating multiple risk factors, which constitutes the novelty of the proposed approach. The model was implemented in an actual construction site as a case study. Also, Particle Swarm Optimization (PSO) and Genetic Algorithm (GA) were employed for comparison purposes. The acquired layout plans showed that the DA provided lower site risk values with feasible solutions for CSLP optimization problems. To validate the results, structured feedback was obtained from 10 experienced project managers and Occupational Health and Safety (OHS) experts, confirming the practical and safety relevance of the optimized layouts. Overall, the proposed DA-based model in this study not only provides feasible solutions for CSLP problems but also integrates comprehensive safety considerations that enable more efficient and safer construction site layouts.

Keywords: construction site layout planning; risk optimization; dragonfly algorithm; dragonfly algorithm-based modeling; model validation

Check for updates

Academic Editor: Pramen P. Shrestha

Received: 15 December 2025
Revised: 17 February 2026
Accepted: 20 February 2026
Published: 28 February 2026

Copyright: © 2026 by the authors. Licensee MDPI, Basel, Switzerland. This article is an open access article distributed under the terms and conditions of the Creative Commons Attribution (CC BY) license.

1. Introduction

Establishing an efficient site layout plan is one of the key activities necessary for the successful execution of a construction project, formally known as construction site layout planning (CSLP). The CSLP has been widely acknowledged as a complex optimization problem. Many studies have been conducted regarding this issue, and comprehensive review papers have also been published that categorize and critically analyze the studies related to this topic [1,2]. Among the various factors, cost and safety parameters are regarded as two significant components in the CSLP problem. However, it is seen that many studies have focused on cost-optimized site layouts rather than safety parameters, even in recent years [3]. Due to risk-related objectives being still less frequently considered as primary optimization targets in CSLP studies, this issue was considered a research gap.

Also, risk mitigation was selected because of its secondary role in the literature, but also to enable a clear and controlled investigation of the Dragonfly Algorithm (DA) within the CSLP context. Before addressing more complex multi-objective trade-offs, DA was first employed in a single-objective risk-based optimization framework to clearly examine the algorithm's search behavior. DA has a simple and flexible structure, which facilitates its application to complex optimization problems such as CSLP. Also, by tuning parameters, it offers effective transition exploration to exploitation behavior in optimization. Additionally, Lévy flight-based random movements enhance exploration in the search space and reduce the probability of premature convergence [4–6]. In the literature, early studies indicate that DA can provide competitive performance compared with commonly used Genetic Algorithms (GAs) and Particle Swarm Optimizations (PSOs) across different problems. It is stated that DA can be capable of producing more robust and consistent solutions in repeated runs, particularly in complex and constrained problem spaces [7–11]. However, it should be noted that these advantages of the DA are not specific to the CSLP problem. Due to the inherent characteristics of the CSLP, DA has the potential to provide effective solutions in this framework.

In early studies, Sing et al. [12] developed a dynamic construction site layout planning model using the Branch and Bound algorithm implemented in LINGO to minimize material handling costs. Abdelalim et al. [13] developed a dynamic construction site layout optimization model integrating cost and safety objectives. Their GA-based approach reduced overall site risk by 28% and material handling costs by 19%. Although Yin [14] made inferences regarding safety risk in the optimization model, the cost parameter was considered the primary objective. However, reducing risk parameters should also be considered as a primary part of the health and safety prevention strategies [15,16]. Moreover, Tao et al. [17] proposed a CSLP-based approach to reduce construction dust-related effects by integrating dust exposure laws and worker distribution into optimization. A multi-objective particle swarm optimization (MOPSO) model was used to minimize dust concentration and transportation cost simultaneously. The results showed that site layout planning can significantly reduce dust-related occupational health risks at a low cost. Yao et al. [18] introduced a multi-objective CSLP model that integrates dust parameters into the optimization process. Dust exposure was modeled with safety risk and transportation cost, and they used NSGA-III with TOPSIS-based decision support to solve the problem. The results showed a certain reduction in environmental pollution, safety risk, and cost simultaneously. Wefki et al. [19] developed a BIM-based multi-objective CSLP model to minimize material transportation cost and maximize site safety. The model uses parametric modeling in Revit to evaluate multiple layout alternatives during early project stages. The case study demonstrated that integrating BIM enables more flexible and accessible multi-objective CSLP decision-making. In general, these studies demonstrate that CSLP can be extended beyond cost minimization by embedding safety and environment-related parameters. However, the adopted safety representations are highly nonuniform and often address specific hazards. This situation limits comparability and makes it difficult to generalize risk-based objectives across projects.

It is well known that a considerable proportion of the high accident rates in construction work occur on construction sites [20,21]. To mitigate these accident rates, several studies have been conducted that incorporate risk issues as a parameter in construction site layout planning. It is known that there is a limited number of safety-focused studies compared to the cost-based optimization. El-Rayes and Khalafallah [22] quantitatively assessed risks associated with crane, hazardous material and route intersections using three performance criteria. Medina-Herrera et al. [23] formulated a risk-based layout optimization model for chemical plant facilities by quantitatively integrating incident probability

and consequence severity into the optimization process. Rezaee et al. [24] addressed CSLP by considering worker behavioral uncertainty in travel path selection. They modeled worker movements and they optimized facility locations by using a GA to minimize travel distance and related safety risks. Abune'meh et al. [25] proposed an integrated framework for optimizing construction site layouts by combining hazard and vulnerability interaction matrices with spatial configuration analysis. El Meouche et al. [26] quantitatively defined risks based on hazard–vulnerability interaction matrices and a spatial risk map based on visibility analysis. Ahumada et al. [15] developed a stochastic framework that integrates quantitative risk assessment with facility layout optimization. Risks associated with explosions, fires, and toxic releases were assessed. Ning et al. [27] proposed a quantitative model for evaluating safety risks in construction site layouts by classifying and quantifying both interaction flows and safety/environmental concerns. The model computes overall site safety levels across alternative layouts. Zavari et al. [28] developed a model that minimizes total traveling distance and enhances safety by quantifying proximity-based relationships among facilities, achieving approximately 20% improvement in overall efficiency compared with conventional layouts. Soliman et al. [29] also considered safety distances and facility conflicts as risk indicators. Risk-based CSLP models usually depend on either flow-based interactions or proximity-based exposure factors. However, few approaches combine multiple interacting risk sources within a single, consistent optimization framework.

From a computational perspective, although the CSLP problem is comprehended as a quadratic assignment problem (QAP) [30–32], it is understood to be difficult to solve due to combinatorial complexity [33,34]. Thus, to find near-optimal solutions, heuristic and metaheuristic algorithms have been mostly used in recent years [35,36]. On the other hand, CSLP problems are considered either static or dynamic site design problems. In static CSLP, the site layout of the facilities is assumed to remain the same throughout the entire construction process. However, dynamic CSLP takes into account different phases of construction work because various facilities serve different functions at different times. Also, Tao et al. [37] proposed a dynamic CSLP model in which construction phases are ordered according to their layout impact, quantified using material transportation data obtained from BIM and scheduling information. A MOPSO algorithm was used to minimize transportation cost and construction noise simultaneously. The study showed that impact-based phase ordering improves layout efficiency compared to static CSLP approaches. From a different point of view, Pham and Pham [38] developed a dynamic multi-objective CSLP model for prefabricated construction projects that accounts for the actual existence time of facilities on-site. The model minimizes tower crane hoisting time and hazard-related risk posed by facilities by using an oMOAHA optimization algorithm, which is a variant of the multi-objective artificial hummingbird algorithm (MOAHA). The results demonstrated that dynamic facility scheduling improves space utilization and safety compared to static and phased CSLP approaches.

To solve the CSLP problem, either single objective or multi-objective, a wide range of metaheuristic algorithms have been employed, including GA [39,40], PSO [41,42], ant colony optimization ACO [43,44] and artificial bee colony algorithms (ABC) [45]. While these methods have shown effectiveness in CSLP problems, they mainly prioritize the cost parameter. In most cases, construction site risks and occupational risk-related factors are either oversimplified or entirely ignored in the modeling process [46–49].

In the optimization process, although some evolutionary methods, such as elitism and mutations, are incorporated to enhance global search capacity, these algorithms still risk premature convergence and entrapment in local optima [3]. Bio-inspired optimization methods have been recently used to overcome such situations. A fuzzy-based bee colony optimization (FBCO) algorithm was developed by Nguyen [50] to solve the CSLP problem

and algorithm parameters were adaptively tuned. The proposed multi-objective CSLP model that simultaneously minimizes facility cost, safety risk, and noise pollution was used in a case study. The results demonstrated that the proposed approach outperformed several metaheuristic methods in achieving safer and more efficient construction site layouts. However, Pham et al. [6] proposed a hybrid optimization model for construction site layout planning that combines DA's exploration with PSO's exploitation. The model determined objectives as transportation cost, noise, and site safety. The results showed that the hybrid approach improves the stability and balance of layout solutions. It is seen that the DA has gained increasing attention due to its adaptability and ability to generate effective solutions [8].

Despite the growing adoption of metaheuristics in the CSLP problems [51–54], only a limited number of studies have considered construction site risk as a primary objective. Additionally, various studies have shown that the proposed models follow different methods in modeling risk parameters based on the site layout problem [50].

It is known that CSLP plays a vital role in ensuring occupational health and safety (OHS) on construction sites. Improper localization of facilities can lead to high worker density, increased material transportation distances, and unsafe proximity between hazardous facilities. To address these issues, this study integrates three safety parameters into the CSLP optimization model: the interaction flow (RF), representing the frequency of worker and material movement; the closeness factor (RS), reflecting environmental and spatial risk exposure between facilities due to proximities; and the crane risk (RC), quantifying the probability of accidents related to crane operations. These parameters collectively establish a quantitative link between layout planning decisions and OHS risk mitigation objectives. In this framework, DA was modified and adapted to address the CSLP problem, and a DA-based optimization model is designated to minimize determined site risks and find optimum solutions. The proposed model was applied to the real construction site as a case study, and the results are compared to PSO and GA algorithms. Also, DA's performance was evaluated using feedback from experienced project managers and occupational health and safety (OHS) specialists. The results demonstrated that the DA-based model produced layouts that have lower risks compared to traditional expert-based layouts, while being applicable to real-world conditions. The methodological framework of the study is shown in Figure 1.

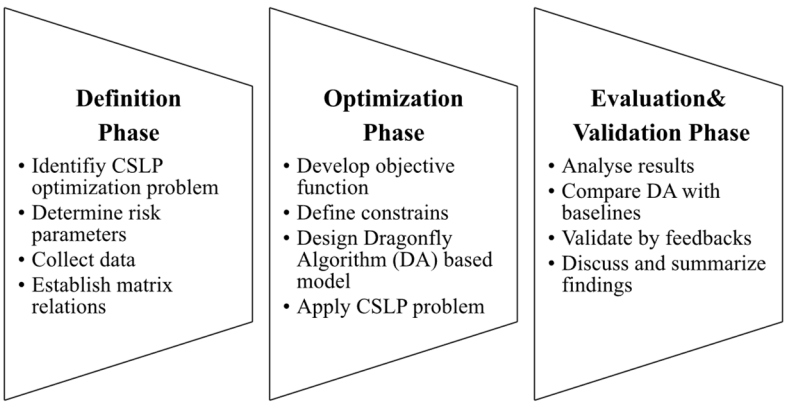


Figure 1. Framework of the study.

2. Methodology

2.1. Site Risks

The risks in the construction site layout planning vary, but the one adopted in this study is taken into consideration to represent safety risks that are directly influenced by

decisions. Although a wide range of safety and risk factors have been identified in early studies, this study focuses on risk mechanisms that can be effectively controlled through the allocational arrangement of temporary facilities. Therefore, determination of site risks, adaptation to the CSLP problem and weight settings can be evaluated in the scope of the risk index system, which systematically represents layout risks in construction sites. First, site risk is defined as accidents arising from spatial relationships and interactions among temporary facilities [2,16,33,55]. Based on this definition, three major factors were used in this study to represent site risk due to the interactions of facilities: interaction flows, the closeness factor, and tower crane influence (Figure 2). These parameters were also chosen because they are more practical and widely accepted for describing facility relationships [6]. Interaction flow-based risk represents the probability of conflicts and accidents due to route intersections and conflict points [13,27,47,56]. Closeness-based risk, reflecting the exposure and interference risks associated with placing facilities too close to or too far from each other, which elevates accident probability [28,57,58]. Crane-related risk, capturing high-severity hazards associated with tower cranes, such as falling objects and lifting operations [22,59]. These parameters are subsequently quantified and they are adopted to risk criteria scales to enable numerical evaluation. The weighting settings of the risk parameters are determined according to the potential consequences of each of them in terms of safety impact. For instance, it is realistic to assign a higher weight coefficient to crane-related risks. However, the weighting values are relative and influenced by the judgments of the responsible site professional. Finally, the quantified risk components are embedded into the optimization process through an aggregated objective function, allowing safety considerations to be directly incorporated into construction site layout planning. However, it should be noted that the selection of risk components, the specific parameter values may be adapted to project conditions and the expert judgment of responsible site professionals. In addition, the overall safety level of the site depends on which types of risks are considered and how many parameters are integrated into the model.

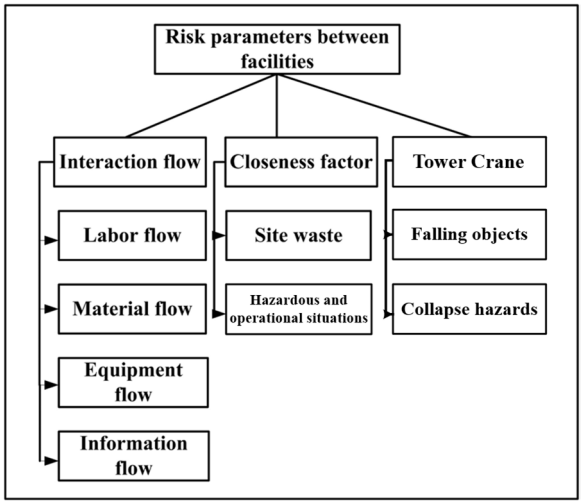


Figure 2. Relationship parameters between facilities.

2.1.1. Interaction Flow

Increasing transportation movement between facilities causes overlaps in routes and creates complications at construction sites [60]. To express the increase in accident probability due to rising intersections [61], an interaction flow is proposed. This interaction flow refers to the movement of labor, materials, equipment, and information between facilities [62]. Labor flow (LF) refers to the number of workers and engineers moving between facilities daily to execute activities. Material flow (MF) refers to the daily trans-

portation of all products, such as raw materials, work-in-progress, and/or finished products, from one facility to another. Equipment flow (EF) refers to the number of tools and equipment (e.g., trucks, mixers and material handling equipment) transferred between facilities [63]. The information flow (IF) is measured as the approximate number of oral communications and documented reports. However, collecting IF data is often impractical in real construction projects [56,64].

2.1.2. Closeness Factor

Environmental risks occur due to the closeness (proximity) of facilities [65]. For example, workers exposed to site waste, such as noise and dust, may experience hearing loss and lung diseases [37,66,67]. Therefore, in terms of construction site safety, facilities should be located further apart from each other. Site waste (SW), hazardous and operational situations (HS), and their associated attributes are considered parameters that affect proximity-related risks. Site risks must be discussed in detail in layout planning. Since this issue requires thorough consideration, categorization was carried out by taking multiple parameters into account. Thus, non-hazardous material waste (MW) such as cement, brick, tile, concrete, ceramics, and metals, construction noise (NO), dust (DU), vibrations (VI) from heavy equipment, and uncomfortable temperature (UT) factors were categorized as site wastes. The use of or presence of explosives and inflammable materials (EIMs), which may cause explosions and fires, high electric voltages (EVs), hazardous chemicals (CHs) and workstation congestion (WC) are identified as hazardous and operational situations (Figure 3). In addition to facilities containing hazardous materials, workstation congestion occurs when facilities with high labor and equipment demand are located in close proximity, if there are multiple activities and high interaction flows. In the proposed framework, congestion-related risks are implicitly reflected through the combined effects of closeness and interaction flow, rather than being modeled as a separate risk parameter. The relationship between facilities was defined as whether there was a risk-related situation associated with these attributes.

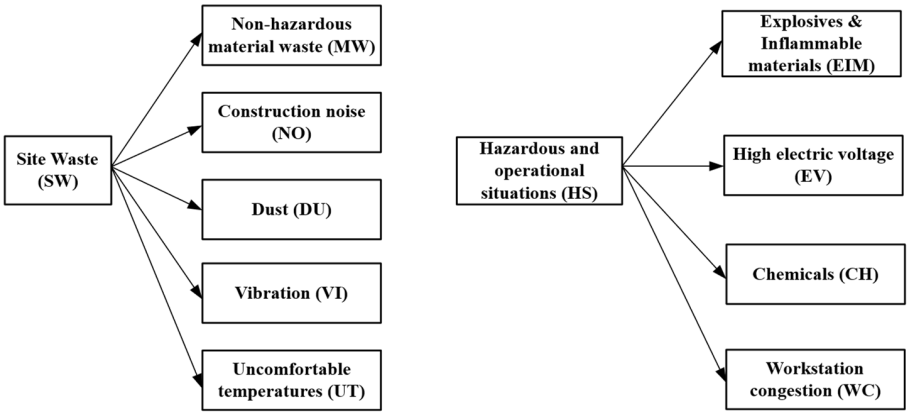


Figure 3. Closeness factor parameters.

2.1.3. Tower Crane

Since tower crane operations are one of the most serious construction activities that can result in fatalities, numerous studies have been conducted on crane safety at construction sites [68–70]. Tower crane-related risks in construction sites primarily arise from falling objects and potential collapse hazards during lifting operations. The severity of these hazards is influenced by several operational conditions, such as limited visibility and hidden work zones during crane operation, as well as interactions between nearby facilities and workers. In the proposed model, risk-specific levels were subsequently aggregated [71]. These conditions are reflected through the distance of crane operation zones and the

closeness of temporary facilities to crane activities, allowing their effect to be represented within a single crane risk component. El-Rayes and Khalafallah [22] developed a model for the CSLP problem that extensively represents crane-related risk. Similarly, in this study, tower crane risks are divided into two zones: the red zone expresses the risky areas due to falling object probability, whereas the green zone expresses the areas where falling objects are not possible. In addition, the risk of crane collapse was ignored because of its low probability of occurrence. The zone separations were formed considering the jib length (J) and shaft width (G) of the tower cranes, which are depicted in Figure 4. The radius of the crane (J + G/2) was considered in determining the risk values between the crane and the facilities. The determined value may pose less risk depending on the movement of personnel and equipment. For example, the damage caused by a falling object onto a gravel storage facility is not the same as the damage caused to a site office facility where personnel are constantly present.

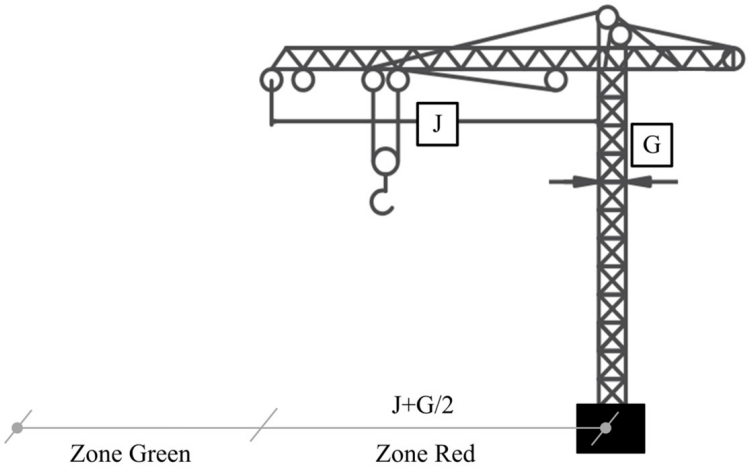


Figure 4. Crane risk zone.

2.2. Defining Risks Between Facilities

Various measurement strategies have been identified to address the risks between facilities, with different scales being used to represent both quantitative and qualitative factors [71,72]. To assess the level of risk for both quantitative and qualitative factors simultaneously, this study designed a risk criterion scale that accounts for risks due to interaction flow and risks arising from the closeness of facilities. Due to the closeness scale being considered the most efficient parameter in previous studies, it is increasing exponentially [34,73]. Also, measuring interaction flow is often impractical [74]. Unlike material, labor, and equipment flows, IF does not represent a physical movement but rather the relative intensity of operational coordination and communication demand between temporary facilities. Moreover, obtaining precise information flow (IF) data is unrealistic [75]. Due to the difficulty of obtaining reliable and continuous quantitative data on construction sites, IF can be represented using qualitative scales based on expert judgment of responsible site professionals. Early studies have employed closeness/intensity scales to capture interaction and coordination requirements between facilities [34,57,76]. Therefore, this study adopts a closeness scale strategy to quantify information flow within the interaction flow [77], as shown in Table 1. This conversion enables the standardization of different flows on a common scale, ensuring consistency on a theoretical basis.

In this table, the scale is set as 'unimportant (UI)', 'not important (NI)', 'important (I)', 'very important (VI)', 'absolutely important (AI)', and 'extremely important (EI)', corresponding to values of 3^0, 3^1, 3^2, 3^3, 3^4, and 3^5, respectively. For example, for an electric generator facility and material storage area containing explosives, when the risk criterion is

classified as 'EI' by an authorized site professional, the closeness scale is assigned a value of '3^5'. Similarly, if the interaction flow quantity ranges between 21% and 40%, it is categorized as 'I', which corresponds to a value of '3^2' in the risk criteria.

Table 1. Risk criteria scale.

Risks Due to Closeness	Level	Quantities for Flows (%)
Unimportant (UI)	3^0	0–1
Not important (NI)	3^1	1–20
Important (I)	3^2	20–40
Very important (VI)	3^3	40–60
Absolutely important (AI)	3^4	60–80
Extremely important (EI)	3^5	80–100

The risk-associated interaction flow increases due to the high amount of labor, material, and equipment movement at the construction site. However, effective verbal communication, regular reporting, real-time information sharing, data exchange, supervision, and efficient organization help to mitigate this risk factor [78]. In addition, greater distances between facilities lead to more road intersections, increasing the risk of accidents. In this study, the risks arising from the interaction flow *RF* between facilities are modeled as illustrated in Equation (1). In this equation, LF_{ij}, MF_{ij}, EF_{ij} and IF_{ij} represent the flow values between facilities (*i*) and (*j*) for labor, material, equipment, and information flow, respectively. *F* denotes the total number of facilities on the site, whereas d_{ij} represents the centralized Euclidean distance between the facilities. Equation (2) provides the calculation for these distances by determining the coordinates of the two facilities (*i* and *j*).

$$RF = \sum_{i=1}^{F-1} \sum_{j=i+1}^{F} \frac{LF_{ij} + MF_{ij} + EF_{ij}}{IF_{ij}} \times d_{ij} \quad (1)$$

$$d_{ij} = \sqrt{(X_j - X_i)^2 + (Y_j - Y_i)^2} \quad (2)$$

The risk associated with the closeness factor (*RS*) is represented in Equation (3), which is based on the acceptance of site waste (*SW*) and hazardous situations (*HS*), which increase the overall site risk, whereas greater distances between facilities reduce this risk. The *SW* and *HS* parameters are calculated as the sum of their respective attributes, as shown in Figure 3.

$$RS = \sum_{i=1}^{F-1} \sum_{j=i+1}^{F} \frac{SW_{ij} + HS_{ij}}{d_{ij}} \quad (3)$$

The risk value associated with the tower crane decreases as the distance between the crane and the facilities increases (Equation (4)).

$$RC = \sum_{i=1}^{CR} \frac{r_{ci}}{d_{ci}} \quad (4)$$

Here, r_{ci} represents the determined risk value for facility (*i*) to crane (*c*), and *CR* denotes the total number of cranes on the site during the optimization process. d_{ci} refers to the Euclidean distance, which is calculated based on the coordinates of each facility relative to all cranes (Equation (5)). The crane radius was also considered in these calculations, as previously defined as J = G + 2 in earlier sections.

$$d_{ci} = \sqrt{(X_{c,j} - X_i)^2 + (Y_{c,j} - Y_i)^2} \quad (5)$$

2.3. Dragonfly Algorithm

The dragonfly algorithm is a metaheuristic swarm optimization model developed by Mirjalili [4], inspired by the behavior of dragonflies. The algorithm simulates the static and dynamic behaviors of dragonfly swarms and has recently gained popularity because of its simplicity and efficiency in solving optimization problems. The static behavior represents the swarm's exploitation capability, which is used for searching for food, whereas the dynamic behavior represents its exploration capability, which is used for avoiding enemies (predators). Like in other swarm-based algorithms, individuals in the swarm follow five principles: separation (S), alignment (A), cohesion (C), food source attraction (F), and enemy avoidance (E). These principles serve as operators, which are calculated using Equations (6)–(10). Additionally, each dragonfly tunes its position based on the status of other adjacent individuals. The neighbourhood radius (r_{ij}) is the Euclidean distance between dragonflies in the swarm, which is calculated by Equation (11).

$$S_i = -\sum_{j=1}^{N} X - X_j \tag{6}$$

$$A_i = \frac{\sum_{j=1}^{N} V_j}{N} \tag{7}$$

$$C_i = \frac{\sum_{j=1}^{N} X_j}{N} - X \tag{8}$$

$$F_i = X^+ - X \tag{9}$$

$$E_i = X^- + X \tag{10}$$

$$r_{ij} = \sqrt{\sum_{k=1}^{d} \left(X_{i,k} - X_{j,k}\right)^2} \tag{11}$$

In these equations, N denotes the number of neighboring dragonflies, X represents the random position of the current dragonfly, and X_j is the random position of the j^{th} neighboring dragonfly. V_j represents the velocity of the j^{th} dragonfly, X^+ refers to the food source, and X^- represents the enemy.

For position updates, the step vector (ΔX) concept, primarily based on the PSO algorithm, is employed. The updated position and velocity are calculated using Equation (12), while the new positions of the dragonflies are computed using Equation (13):

$$\Delta X_{t+1} = (s \times S_i + a \times A_i + c \times C_i + f \times F_i + e \times E_i) + w \times \Delta X_t \tag{12}$$

$$X_{t+1} = X_t + \Delta X_{t+1} \tag{13}$$

Here s, a, c, f, and e are coefficients indicating that the weights depend on the behavior of the dragonfly swarm. Where i refers to the i^{th} dragonfly, w is the inertia weight of the current swarm position, and t is the iteration counter.

If a dragonfly has no neighbors within its neighborhood radius, its position is updated using the Lévy flight mechanism [45,79], which enhances randomness and global search capability. The new positions are calculated using Equations (14)–(16):

$$\sigma = \left(\frac{\gamma(1+\beta) \times \sin(\frac{\pi\beta}{2})}{\gamma(\frac{1+\beta}{2}) \times \beta \times 2^{(\frac{\beta-1}{2})}}\right)^{1/\beta} \tag{14}$$

$$Lévy(x) = 0.01 \times \frac{r_1 \times \sigma}{|r_2|^{1/\beta}} \tag{15}$$

$$X_{t+1} = X_t + Lévy(d) \times X_t \tag{16}$$

In these equations, r_1 and r_2 are two random variables in the range [0, 1] and β is a constant value that varies between [0.5, 1.5] depending on the static or dynamic behavior of the dragonfly swarm.

3. Proposed Model

In this study, the proposed approach for modeling is based on the use of matrices to depict the risk parameters between facilities. The matrix-based solution approach of the DA provides a framework that can be easily applied to CSLP problems and customized according to different project requirements. In the model, the coordinates of the temporary facilities are defined as variables. Each column of the matrix is depicted as the centralized coordinates of the number of temporary facilities (f), which also correspond to a potential solution (X_1, Y_1, X_2, Y_2, …, X_f, Y_f). The population size (n) of the matrix is defined as the number of potential solutions in the search space. This coding system has been preferred for representing and solving CSLP problems [80]. The XY_{nxf} population matrix (Figure 5) is generated randomly for each pair of facility coordinates, ensuring that the coordinates remain within the site boundaries.

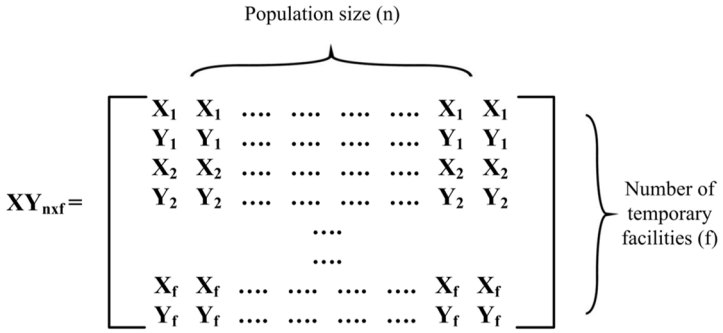


Figure 5. Facility coordinates as population matrix.

3.1. Objective Function

This study identified three objective functions. However, incorporating multiple objective functions increases the problem's complexity, resulting in a prolonged optimization process. To reduce this complexity and facilitate the evaluation of the safety factor at the construction site, three methods are recommended: combining objectives into a performance criterion, obtaining a solution by turning the objective into constraints, and the dominant Pareto-based optimal method [81]. Considering the structure of the problem, the objective functions are gathered into a single objective function within the performance criterion [76,82]. Consequently, the parameters representing risks due to interaction flow (*RF*), the closeness factor (*RS*), and risks associated with cranes (*RC*) were consolidated using relative weight coefficients (w_1, w_2, w_3). These coefficients can be obtained from historical safety records and data on fatalities or injuries from previous projects, as reported by companies [22]. The objective function, which considers minimizing the total risk (*TR*), is presented in Equation (17). In this study, the weight coefficients were assigned as w_1 = 0.2 for the interaction flow parameter, w_2 = 0.2 for the closeness factor parameter and w_3 = 0.6 for the tower crane parameter. The weight coefficients were assigned to reflect the relative dominance of different risks in the construction site from a safety-impact perspective. Tower crane risks are mostly associated with fatal and catastrophic outcomes, which indicates a more dominant contribution to the total risk function. For this reason, a higher weight value was assigned to the crane risk factor to reflect its intense influence on overall site safety compared to the interaction flow and closeness factor risks. However, the weighting values are influenced by the judgments and experiences of site managers or decision-makers who are responsible for construction site planning, which means that

different weighting values lead to different layout solutions. The total weight was leveled in this study among the parameters according to the assumption that the tower crane would pose a higher risk factor.

The weighting reflects the general industry perception of risk priorities in construction projects and is consistent with the Ning et al. [82], which has a similar total risk equation. However, if the safety records or risk priorities differ across construction sites, the weight coefficients can be adjusted accordingly. This naturally leads to site-specific variations in the objective function, reflecting different managerial perceptions of risk. However, minor variations within realistic ranges (±5–10%) were also tested and did not significantly affect the overall layout structure. This situation also depicts the robustness of the weighting.

$$TR = \sum_{i=1}^{N-1} \sum_{j=i+1}^{N} \left(\left(\frac{LF_{ij} + MF_{ij} + EF_{ij}}{IF_{ij}} \times d_{ij} \times w_1 \right) + \left(\frac{SW_{ij} + HS_{ij}}{d_{ij}} \times w_2 \right) \right) + \sum_{i=1}^{CR} \left(\frac{r_{ci}}{d_{ci}} \right) \times w_3 \quad (17)$$

3.2. Constraints

At a construction site, areas such as the main construction area, tower cranes, transportation roadways, obstacles due to land characteristics, etc., are considered unoccupied areas or fixed facilities [57]. Therefore, for the coordinates of temporary facilities, the obtained results must remain within the determined search space for the algorithm. In this study, the solutions obtained during the optimization process are constrained to lie outside the coordinate values of the structures classified as fixed facilities in the model.

In optimization, the minimum total risk is achieved by determining the coordinates in the search space. However, when seeking the optimal solution, the algorithm may place the coordinates of the facilities outside the site boundaries, or the obtained coordinates may lead to overlap [25]. Therefore, the results must satisfy the boundary (Equations (18)–(21)) and overlap (Equations (22) and (23)) conditions to obtain a feasible site layout. Figure 6 illustrates the boundary and overlap conditions for facilities within the site area.

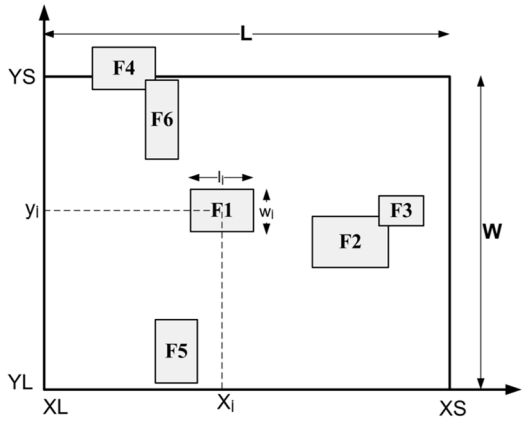


Figure 6. Boundary and overlap conditions.

$$XL + \frac{l_i}{2} \leq X_i \quad (18)$$

$$X_i + \frac{l_i}{2} \leq XS \quad (19)$$

$$YL + \frac{w_i}{2} \leq Y_i \quad (20)$$

$$Y_i + \frac{w_i}{2} \leq YS \quad (21)$$

$$\frac{l_i + l_j}{2} \leq |X_i - X_j| \quad (22)$$

$$\frac{w_i + w_j}{2} \leq |Y_i - Y_j| \tag{23}$$

Here, the lower and upper bounds of the site area are depicted as *XL*, *YL*, *XS*, and *YS* in the *X* and *Y* directions, respectively. *l* and *w* represent the length and width of the facilities (*i*) or (*j*). X_i, X_j , and Y_i, Y_j denote the center coordinates of the specified facilities.

Additionally, the model's results depend on the number of constraints and how they are applied to the model [83]. To obtain acceptable results, this study incorporates safe distances as suggested by Sanad et al. [72]. These distances refer to extra areas added to the physical area of the facilities that mitigate the risks arising from the movement of personnel, materials, and equipment operations [71]. It is recommended that the distances should be consistent with regulations such as fall prevention measures [84]. For this reason, the areas of temporary facilities are expanded by 20% as a conservative safety distance in this study. Therefore, the dimensions of the facilities are extended in both the *X* and *Y* directions during the optimization process to standardize modeling across facilities (Figure 7). However, the safety distance value can be changed or adjusted by the responsible site professional.

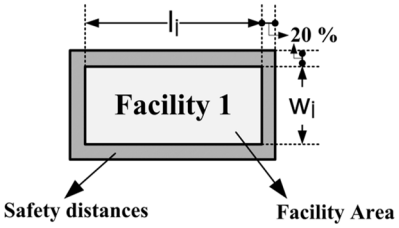


Figure 7. Extended dimensions of temporary facilities.

3.3. DA Implementation

In optimization problems, it is possible to adapt almost all metaheuristics to any problem. It has also been known that bio-inspired metaheuristics are widely applied to numerous optimization problems; however, this situation creates conflict for fostering a problematic paradigm in the comprehension of these algorithms [85]. In our study, DA was evaluated not for its bio-inspired appeal but for its ability to address the complexities of CSLP. The design of the DA for the CSLP problem is structured by the specific characteristics of CSLP, which is a multi-factorial, spatially constrained, and nonlinear optimization problem. While satisfying boundary and overlap conditions simultaneously in feasible solutions, it is essential to avoid trapping local optima. The behavioral mechanisms of the DA are particularly suitable for this purpose, as strong exploration in early iterations enables the identification of promising layout regions, while intensified exploitation in later iterations allows adjustments of facility locations without violating boundary and overlap constraints. Therefore, the decision to employ the DA stems from empirical evidence and practical considerations, such as its capability in balancing exploration and exploitation, fast convergence, and effectiveness in constrained problems. Accordingly, the parameters and update strategies are configured to reflect DA's search behavior, ensuring convergence towards promising search space areas and feasible layout solutions.

Regarding coefficients, the inertia weight (*w*) is gradually reduced during the iterative process to provide a smooth transition from exploration to exploitation. The separation coefficient (*s*) is kept constant, whereas the alignment (*a*) and cohesion (*c*) coefficients are adaptively adjusted in opposite directions to reflect the global search diversity and local solution refinement. Setting the sum of *s*, *a*, and *c* equal to unity ensures balanced swarm behavior and prevents any single interaction mechanism from dominating the search process. In addition, the food (*f*) and enemy (*e*) coefficients are assigned equal values to maintain operational effectiveness of the *s*, *a*, and *c* parameters. This adjustment prevents the search process from getting stuck at a single point or avoiding specific areas.

Nevertheless, it should be noted that to balance exploration and exploitation, the swarming factors (s, a, c, f, e, and w) can adaptively tune. Variations in the tuning of behavioral coefficients may influence the search dynamics and convergence tendencies of the algorithm, without implying deterministic effects on the final layout solutions.

From the convergence behavior and stability, the determined coefficient update mechanism enables a gradual transition from exploration to exploitation. This mechanism is based on the behavior of dragonflies, which promotes convergence because it is assumed that dragonflies tend to see more dragonflies to adjust the flying path during the optimization process [4]. During the iterative process, the behavior of the DA population finds feasible layout areas while avoiding premature convergence. Overall, the proposed algorithm demonstrates reliable convergence characteristics and stable performance in addressing the complexities of CSLP.

In addition, minimizing the computational load is crucial due to the complexity of the solutions. As a fast-tracking algorithm, the DA has already been applied to solve problems in various fields [86,87]. Compared to other bio-inspired metaheuristics, the DA is preferred for its efficient exploration and convergence mechanisms [88]. The results of the benchmark tests demonstrate the superior performance of DA over GWO, PSO, and GA [11]. Additionally, the DA performs better than its variants do in global optimization problems [89]. This suggests that adapting the DA to the current problem with minor modifications may produce better results.

In our model, each column of the XY_{nxf} population matrix represents an alternative solution. The coordinates are coded such that every possible solution is represented by a dragonfly in the algorithm's search space. Figure 8 shows the behavior of the "n" dragonflies in the search space, where they seek the best solution (i.e., best layout) by avoiding the enemy (predator) and moving toward the food source (prey).

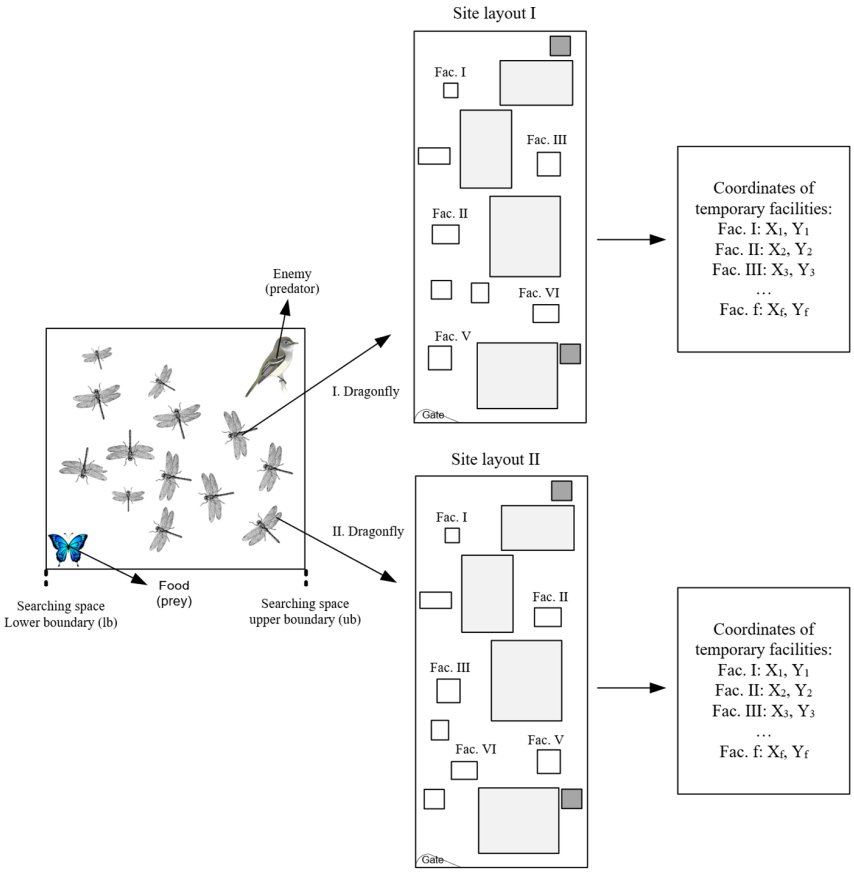


Figure 8. Dragonflies in the swarm as a representation of potential solutions.

The pseudo-code and flowchart of the DA-based model are shown in Algorithm 1 and Figure 9, respectively. The corresponding equations are taken from Section 3.3 and implemented in the CSLP problem.

Algorithm 1. Pseudo-code of the DA-based algorithm

```
Input specifications on construction site and facilities
Input relations between facilities
Initialization set of parameters (maximum iteration, maximum number of search agents)
Initialize the dragonflies population Xi (i = 1,2, . . ., n)
Initialize step vectors ΔXi (i = 1,2, . . ., n)
Check boundary and overlap conditions in the construction site
While maximum iterations not satisfied
Calculate the objective values of all dragonflies
Update food source (F) and enemy (E) values
Update w, s, a, c, e, f coefficients
Calculate S, A, C and F, E values
Update neighborhood radius (r)
    if a dragonfly has at least one dragonfly in the neighborhood
        Update step vector (ΔX)
        Update position vector (X)
            Check boundary and overlap conditions in the construction site
            if there is a violation in boundary or overlap conditions
            Restrict relevant ΔX value
            end if
    else
        Update position vector (X) by using Lévy Flight
            if there is a violation in boundary or overlap conditions
            Restrict relevant ΔX value
            end if
    end if
Check the new positions based on the boundaries of variables
End while
```

To utilize the model, the following information must first be provided: the construction site boundaries, the lengths and widths of temporary facilities, the structures within the construction process (considered fixed facilities), and the length, width, and coordinates (x, y) of the tower cranes. The algorithm begins by initializing the population size (XY) and step size (ΔX), ensuring that randomly generated coordinate values do not overlap and remain within the site boundaries. The population sizes of "n" dragonflies are expressed as X_1, X_2, X_3, . . ., and X_n. For example, dragonfly X_1 is a particle with dimensions of x_1, y_1, x_2, y_2, ... x_f, y_f coordinates. Thus, each dragonfly contains "temporary facilities *2" coordinate values. The same coding system applies to the ΔX procedure. The objective values of the coordinate values produced in the first iteration are calculated within themselves. The S, A, C, F and E values are calculated using the w, s, a, c, e, and f coefficients that are entered first and then updated via iterations. While adjusting the coefficient values here, the inertia coefficient (w) was reduced in direct proportion to the increase in the number of iterations, from 0.9 to 0.4 values, to simulate the transition features of the algorithm from exploration to exploitation. The value of the separation coefficient (s) was kept constant at 0.2, the alignment coefficient (a) was reduced between 0.7 and 0.1 values inversely proportional to

the number of iterations, and the cohesion (c) coefficient was increased between 0.1 and 0.7 values in direct proportion to the number of iterations. The coefficients of food and enemy factors (f and e, respectively) were determined to be 1 [4,7]. In addition, the sum of the coefficients s, a, s and c being equal to 1 showed that the solutions were effective by ensuring a balanced behavioral interaction among separation, alignment, and cohesion coefficients, preventing any single behavior from dominating. These adaptive behaviors were expressed in Equations (24)–(26).

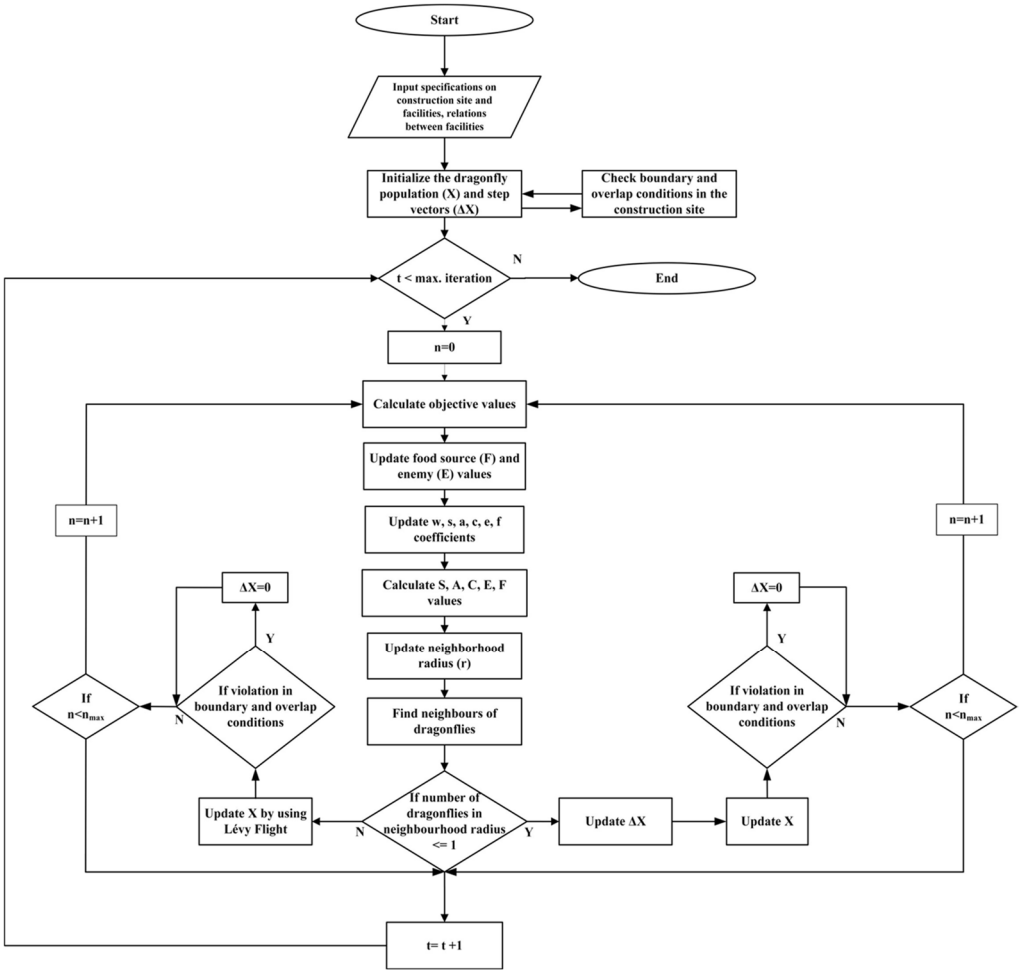


Figure 9. The flowchart of the DA-based algorithm.

$$w_{(t)} = w_{start} - (w_{end} - w_{min}) + \frac{t}{T} \tag{24}$$

$$a_{(t)} = a_{start} - (a_{end} - a_{min}) + \frac{t}{T} \tag{25}$$

$$c_{(t)} = c_{start} - (c_{end} - c_{min}) + \frac{t}{T} \tag{26}$$

where t represents the current iteration and T denotes the total number of iterations.

During the algorithm's repetitive search process, the dragonflies are required to update their positions relative to each other and reach the best solution by increasing their neighbourhood radius (r) until they reach the maximum number of iterations. Here, ub refers to the upper boundaries of the search space in the planar dimension, and lb refers to its lower boundaries (Figure 8). The maximum number of iterations can be determined by the user.

4. Case Study

An extensive lifestyle resort project, featuring commercial and recreational facilities, including a residential building, cinema, theatre, shopping center, and fitness center, was selected as a case study. This case study data was obtained from the actual site layout and design documentation of the project. The data regarding locations and coordinates were also extracted from architectural drawings and topographic surveys. Figure 10 illustrates the construction phase and visual representation of the completed project, which consists of a total of 843 residences and 53 commercial areas.



Figure 10. The project used as a case study.

The project has an approximate building footprint area of 3000 m^2 and is located within a 20,700 m^2 construction site area and has an approximate total floor area of 150,000 m^2. The site plan of the project, shown in Figure 11, features three tower blocks: Block B with 31 storeys, Block A2 with 37 storeys, and Block A1 with 38 storeys, reaching a maximum height of 136 m. Block F is a porch structure planned for construction after the completion of the other blocks.

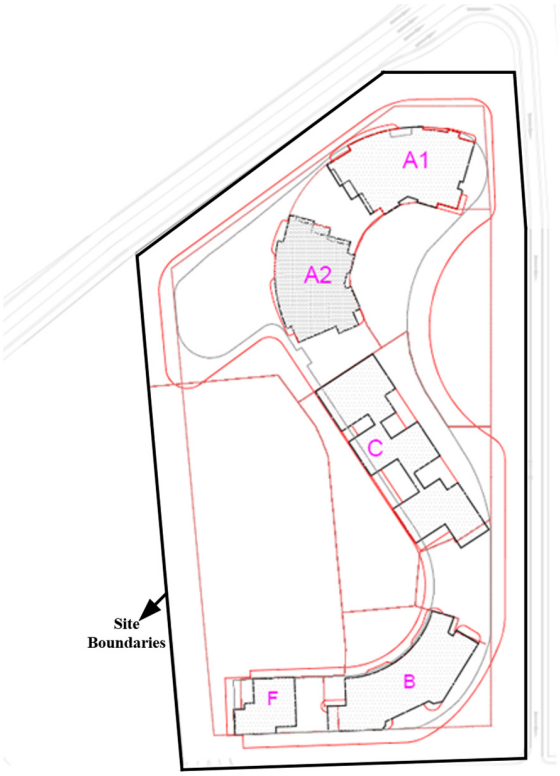


Figure 11. The site layout plan of the project.

For all buildings to be constructed, the outermost points of their actual shapes are determined, and a rectangle is drawn with those points as the corners. This assumption ensures minimum area loss for representing building areas. There are two reasons for taking into consideration the buildings as rectangular shapes: (1) in terms of health and safety measures, fall accidents can be prevented by locating temporary facilities distant from fixed facilities [90], (2) to decrease the optimization duration. In addition, gaps (distances) created by the rectangular shape provide safe travel for site personnel.

The construction project is positioned within a coordinate system where the exterior points of the site intersect at the (0, 0) point. The coordinates of the corner points defining the site boundaries are determined as (14, 0), (116, 3.5), (115, 165), (112, 208), (73.5, 208), and (0, 154). In this study, the construction phase considered two cranes that can reach specific points of the four blocks, which are fixed facilities, while eight temporary facilities are located. It should also be noted that the location of concrete pumping facilities is an important decision in construction site layout planning. Due to the scope of this study focusing on static site layout optimization, the concrete pump was not considered as a fixed or temporary facility, as it represents a high-frequency, short-term, and operation-dependent resource whose position varies throughout the construction process. For the tower crane, the horizontal operational range is set as 80 m (J + G/2), and this distance is accepted as the radius of the crane. The buildings to be constructed are represented in a rectangular shape, with site boundaries and roadways depicted in Figure 12. The nomenclature and specifications of the facilities are presented in Table 2.

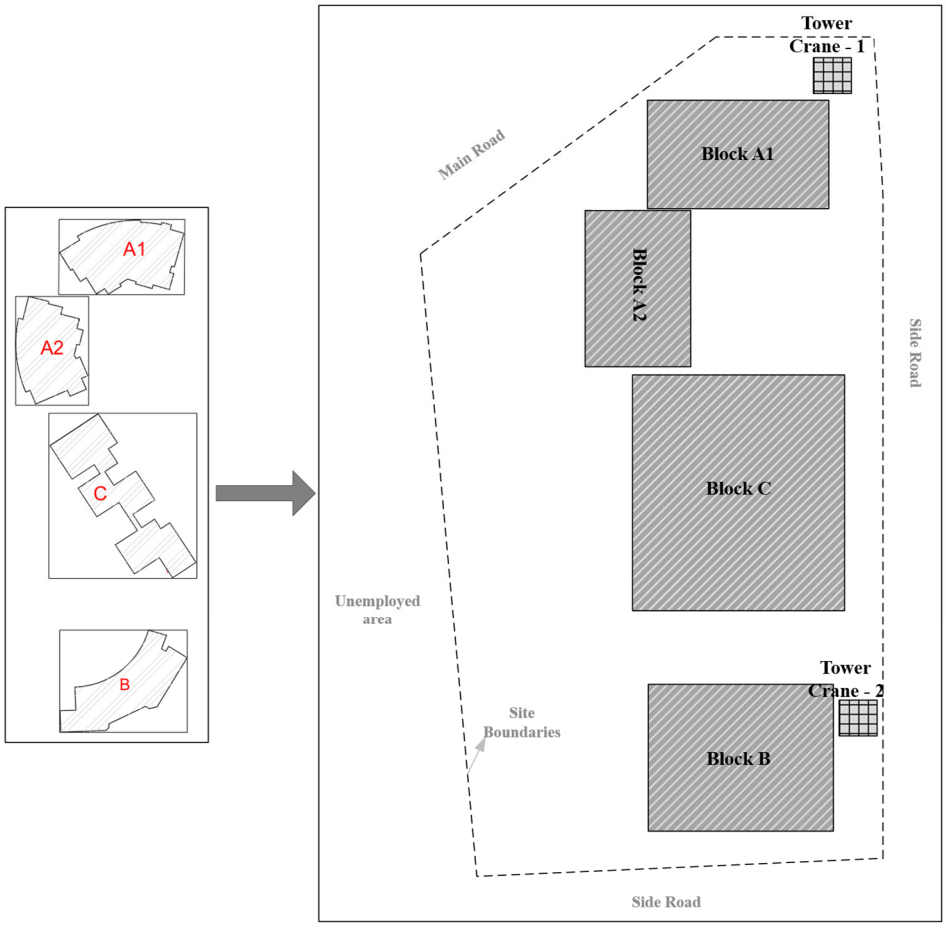


Figure 12. Representation of the construction site.

Table 2. Specifications of facilities.

Facility Name	Facility Assignment	Facility Length (m)	Facility Width (m)	Safety- Distanced Length (m)	Safety-Distanced Width (m)	Facility Location (x, y)
Block-A1	F_{b-1}	44	26	-	-	(80, 180)
Block-A2	F_{b-2}	25	38	-	-	(56, 148)
Block-C	F_{b-3}	52	57	-	-	(81, 96.5)
Block-B	F_{b-4}	36	45	-	-	(77, 30)
Tower Crane-1	F_{c-1}	10	10	-	-	(102, 200)
Tower Crane-2	F_{c-2}	10	10	-	-	(107, 41)
Gate	G	15	3.5	-	-	(21, 3)
Cement storage	F_1	8	8	10	10	unspecified
Sand storage	F_2	10	10	12	12	unspecified
Formwork storage	F_3	12	12	15	15	unspecified
Decoration material storage	F_4	12	8	15	10	unspecified
Waste area	F_5	20	10	24	12	unspecified
Rebar bending workshop	F_6	10	10	12	12	unspecified
Carpentry workshop	F_7	15	10	18	12	unspecified
Electric generator	F_8	3	3	4	4	unspecified

Additionally, data (both numerical and verbal) on the daily average and the maximum number of personnel traveling between the facilities, the number of traveling for material transport and the amount of equipment transport were determined by work schedules, material procurements and heavy equipment work plans. This dataset was gathered through on-site observations and expert assessments conducted with the assistance of the project management team. The labor flow values (in terms of person/day) between facilities are converted according to the risk criteria scale and given in Table 3. The material, equipment and information matrices were also created and presented in Supplementary File as Tables S1–S3, respectively. Similarly, each matrix represents pairwise interactions among facilities, where no self-interaction occurs in diagonal elements, and off-diagonal values denote the intensity or risk level between facilities.

Table 3. Labor flow values between facilities.

Facilities	F_1	F_2	F_3	F_4	F_5	F_6	F_7	F_8	F_{b-1}	F_{b-2}	F_{b-3}	F_{b-4}	F_{c-1}	F_{c-2}
F_1	0	VI	UI	UI	UI	UI	UI	UI	EI	EI	EI	EI	EI	EI
F_2		0	UI	VI	I	UI	UI	UI	EI	EI	EI	EI	EI	EI
F_3			0	I	I	VI	EI	UI	EI	EI	EI	EI	EI	EI
F_4				0	AI	UI	VI	UI	EI	EI	EI	EI	EI	EI
F_5					0	UI	I	UI	EI	EI	EI	EI	EI	EI
F_6						0	UI	UI	EI	EI	EI	EI	EI	EI
F_7							0	UI	EI	EI	EI	EI	EI	EI
F_8								0	EI	EI	EI	EI	EI	EI
F_{b-1}									0	EI	EI	EI	EI	EI
F_{b-2}										0	EI	EI	EI	EI
F_{b-3}											0	EI	EI	EI
F_{b-4}												0	EI	EI
F_{c-1}													0	EI
F_{c-2}														0

Since the closeness of facilities to each other increases the risk within the construction site, they should be located as far away from each other as possible. The relationships among facilities are obtained based on the knowledge and experience of the project manager, or who is responsible for deciding the locations of the facilities. There is a subjective and verbal description of the relationship between the two facilities which includes both qualitative and quantitative aspects. For instance, electric generator–waste area closeness possesses more risk (VI in risk criteria scale) than electric generator–sand storage (NI in risk criteria scale). Non-hazardous wastes, noise, dust, vibration, and uncomfortable temperatures are considered construction site waste parameters, while facilities containing explosive and inflammable materials, high electrical voltages, or hazardous chemicals are

classified as hazardous materials. Risk matrices are defined for nine parameters and the closeness factor between facilities for noise is given (Table 4). Other parameters' matrices are given in Supplementary File as Tables S4–S10 for the closeness factor.

Table 4. The closeness factor between facilities for the noise parameter.

Facilities	F_1	F_2	F_3	F_4	F_5	F_6	F_7	F_8	F_{b-1}	F_{b-2}	F_{b-3}	F_{b-4}	F_{c-1}	F_{c-2}
F_1	0	UI	UI	UI	UI	NI	NI	NI	UI	UI	UI	UI	UI	UI
F_2		0	UI	UI	UI	NI	NI	NI	UI	UI	UI	UI	UI	UI
F_3			0	UI	UI	NI	NI	NI	UI	UI	UI	UI	UI	UI
F_4				0	UI	NI	NI	NI	UI	UI	UI	UI	UI	UI
F_5					0	NI	NI	NI	UI	UI	UI	UI	UI	UI
F_6						0	EI	NI	EI	EI	EI	EI	EI	EI
F_7							0	EI	EI	EI	EI	EI	EI	EI
F_8								0	EI	EI	EI	EI	EI	EI
F_{b-1}									0	EI	EI	EI	EI	EI
F_{b-2}										0	EI	EI	EI	EI
F_{b-3}											0	EI	EI	EI
F_{b-4}												0	EI	EI
F_{c-1}													0	EI
F_{c-2}														0

For the tower crane parameter, crane specifications were taken from the project's equipment plans and manufacturer data sheets. Also, collected data were verified with the site's Health and Safety reports and the project's schedule. Based on the data, risk matrices are determined and shown in Table 5. To minimize the risk of accidents involving falling objects, the locations of temporary facilities were presumed to be in the red zone. Specifically, in areas with a high density of laborers, it is essential that temporary facilities are situated beyond the crane's operational range [91].

Table 5. Risk matrices that emerged in facilities.

Facilities/Cranes	F_1	F_2	F_3	F_4	F_5	F_6	F_7	F_8	F_{b-1}	F_{b-2}	F_{b-3}	F_{b-4}	F_{c-1}	F_{c-2}
F_{c-1}	EI	EI	EI	EI	EI	EI	EI	EI	EI	EI	EI	EI	0	0
F_{c-2}	EI	EI	EI	EI	EI	EI	EI	EI	EI	EI	EI	EI	0	0

5. Results

The population size (n) was constant for each level (50, 100, and 200) and the number of iterations was gradually increased to 50, 100, and 200, due to the expectations for improved results [92] and the possibility of better site layouts. For each population value and iteration count, the optimization is run 25 times (all results are given in the Supplementary File as Tables S11–S13). The best results obtained were recorded, and the combinations of these results were compared (Table 6). MATLAB software (R2021b version) was preferred for the optimization in this study. The time required to solve the problem ranged from 52 to 943 s (s) on average, depending on the population size and the number of iterations. This includes the CPU time and display of facilities on a 2.5 GHz Intel(R) Core (TM) i7-4710HQ CPU with 16 GB RAM personal computer. The minimum values were evaluated as the best value in the running process in the optimization to determine the best site layout.

The best value obtained was 5.270 with a population size of 200 and 200 iterations. The convergence curves are shown for the iteration values run in optimization and the corresponding population sizes (Figure 13). Each curve shows the progression of the best risk value over iterations. The results indicate that the algorithm achieves rapid improvements in the early stages (first 50–75 iterations), followed by gradual convergence. This behavior demonstrates the DA's efficiency and improvement in the solutions (from the first to the last iteration), proving that the DA is applicable to real CSLP problems. It is

also observed that the DA finds the optimum solution by transitioning from exploration to exploitation without being trapped in local optima. Due to constraints forcing the algorithm to find reasonable coordinates within the construction site, the solutions obtained did not exhibit significant changes in the site layout plan after a certain number of iterations. The site layout of the temporary facilities that are determined by the best value is shown in Figure 14, with their coordinates provided in Table 7.

Table 6. Results of DA optimization.

	Number of Population (n)					
	50		100		200	
Number of Iterations	Best Value	Duration (s)	Best Value	Duration (s)	Best Value	Duration (s)
50	5.573	52.07	5.407	102.68	5.428	312.75
100	5.531	97.95	5.353	215.18	5.340	604.35
200	5.471	174	5.434	385.43	5.270	1056.71

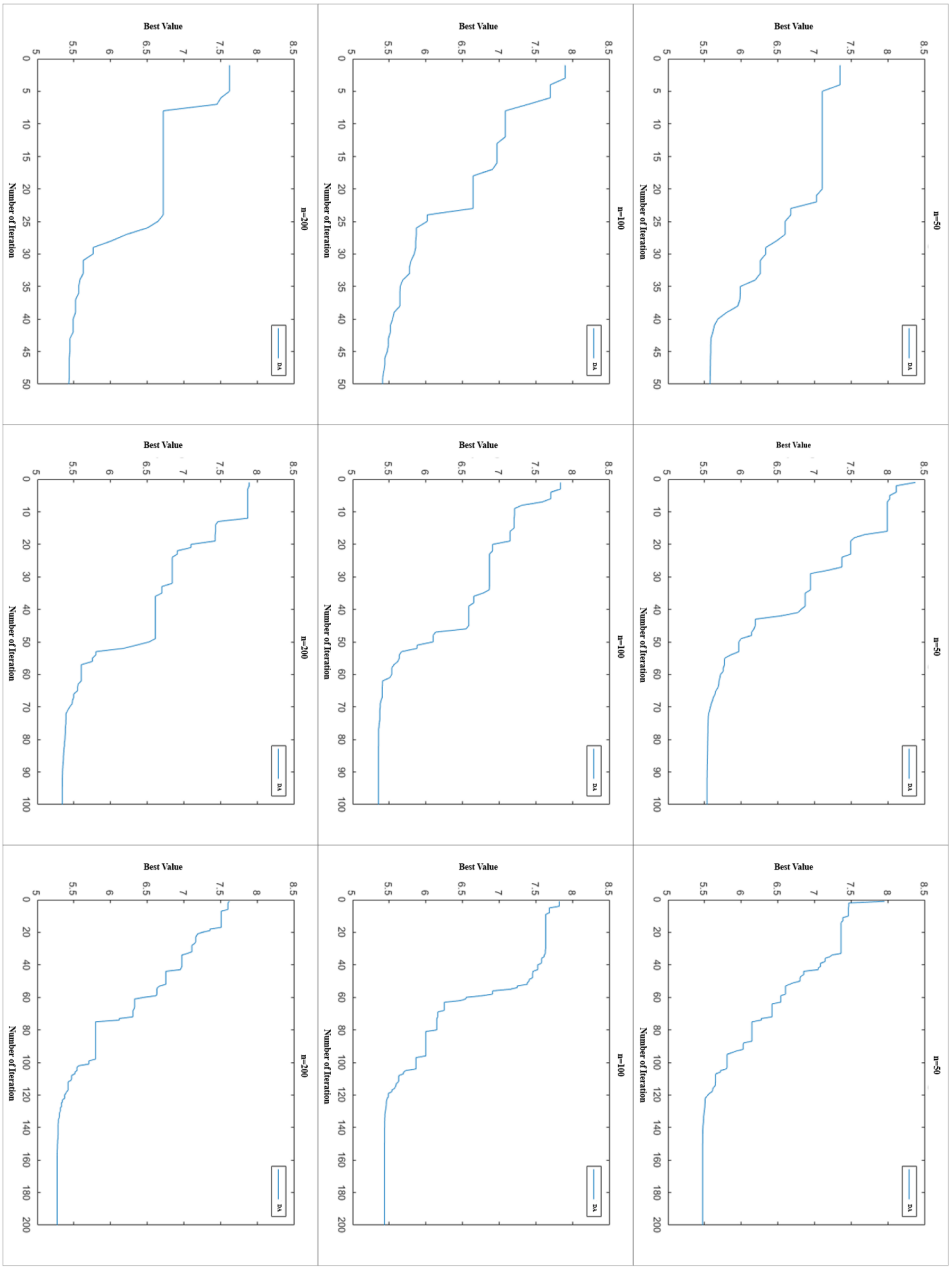


Figure 13. Convergence plots of the DA-based model.

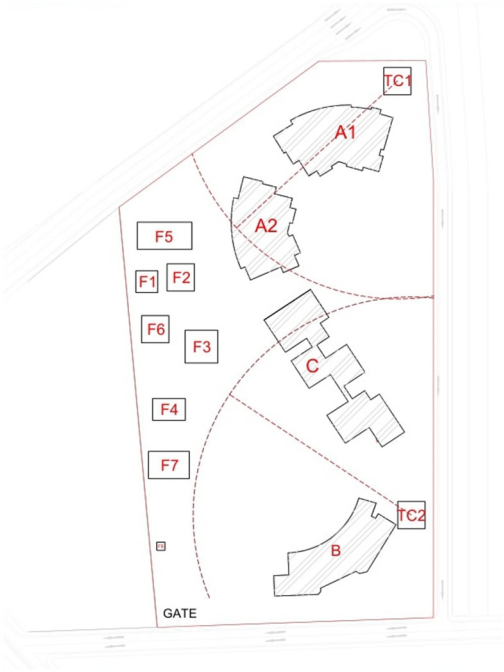


Figure 14. Site layout for the best value of the algorithm.

Table 7. Coordinates of the temporary facilities obtained from optimization results.

Facilities	Facility Coordinates (x, y)
Cement storage (F1)	(10.20, 127.18)
Sand storage (F2)	(22.62, 128.74)
Formwork storage (F3)	(30.20, 103.36)
Decoration material storage (F4)	(18.31, 80.34)
Waste area (F5)	(16.7, 144.02)
Rebar bending shop (F6)	(13.27, 109.75)
Carpentry workshop (F7)	(18.49, 60.01)
Electric generator (F8)	(15.33, 30.17)

The following results were determined:

- It was observed that for a population size of 50, there were no significant differences in the optimum solution between the 50th and 100th iterations. It can be concluded that a population size of 50 was insufficient for exploring the search space. However, by the 200th iteration, the facilities begin to move further apart, indicating reduced risk.
- Increasing the population size from 50 to 100 and then to 200 demonstrated that acceptable layout plans could be achieved by increasing only the population size without changing the number of iterations, even with a constant 50 iterations.
- For a population size of 100, an increasing population (50, 100, and 200) caused significant changes in the facility layout.
- When the population size was increased to 200, lower risk values were achieved as the number of iterations increased, resulting in the two best alternative layout plans. The minimum values obtained from solutions with population sizes of 100 and 100 iterations were found to be nearly identical to those obtained with population sizes of 200 and 100 iterations.
- The time taken to reach the best value is 1056.71 s (16 min and 67 s). Additionally, the second- and third-best results were achieved at 604.35 and 215.18 s, respectively. Since there are no significant differences in facility layouts at the construction site, the result

of 5.353, achieved with a population size of 100 and 100 iterations, could be considered preferable for practical applications in a field study.

- The standard deviation values were calculated from multiple runs of the model across all population sizes. For population sizes of 50, 100, and 200, they are between 0.318 and 0.36, 0.28 and 0.234, 0.216 and 0.172, respectively (determined box plots are given in Supplementary File as Figures S1–S3). It is seen that results deviated reasonably from the mean, suggesting that the dragonflies' behavior in the search space was acceptable.

6. Discussion

To validate the results, PSO and GA algorithms were employed for the same CSLP case study. The results of the best values obtained by the PSO and GA algorithms are presented in Table 8, and convergence plots of these best results are depicted in Figure 15 for populations of 50, 100, and 200 with 50, 100, and 200 iterations, respectively. It was observed that the results of PSO and GA were slightly inferior to those of DA.

Table 8. Results of the best values of PSO and GA.

	Number of Population (n)					
	50		100		200	
Number of Iterations	**PSO**	**GA**	**PSO**	**GA**	**PSO**	**GA**
50	6.092	6.468	5.755	6.246	5.695	6.317
100	5.816	5.955	5.720	5.859	5.485	5.698
200	5.702	6.405	5.630	5.754	5.432	5.510

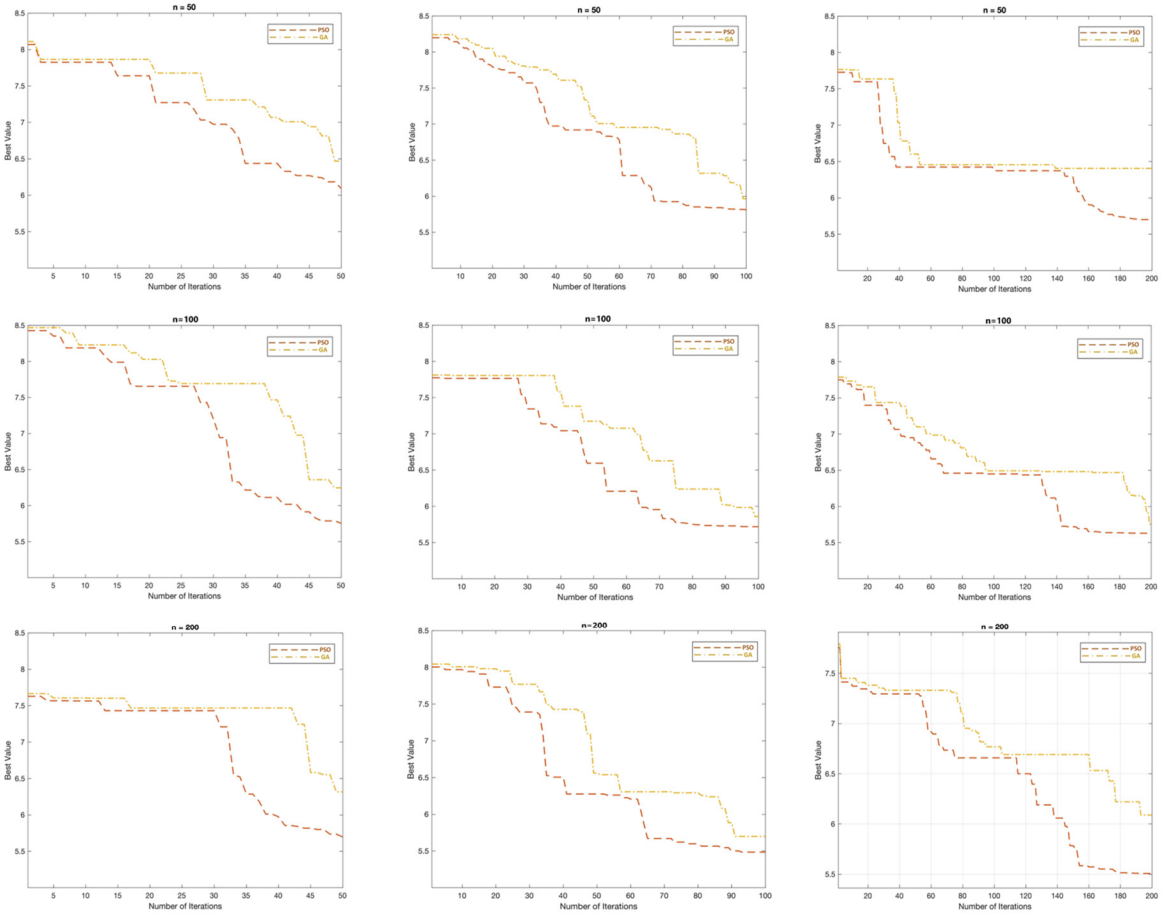


Figure 15. Convergence plots of PSO and GA optimization results.

In addition to the validation, an expert assessment process was conducted. In this scope, the layout plans obtained from the optimization process were shared with participants, who are professionals from various occupational groups who had experience placing facilities on construction site projects of a similar scale, and their feedback was requested. The purpose of this feedback was to determine whether professionals who had experienced risk scenarios in the CSLP problem found the results obtained with the DA to be satisfactory or better than their own, or to provide suggestions for improving the study. For this reason, feedback was collected from 10 participants, and the professions, roles, and sectors of the experts were shown in Table 9. All the participants had 3 to 25 years of experience in their respective fields. In addition, it is already expected that, based on professionals' knowledge and experience in site management and a health and safety perspective, different layout plans may result. The participant questions were given in Table 10.

Table 9. Participant information.

Participant No.	Profession	Position/Role	Sector
1	Civil Engineer (M.Sc)	Technical Specialist	Public
2	Civil Engineer	Site Manager (Superintendent)	Private
3	Mechanical Engineer	Field Engineer	Private
4	Civil Engineer (M.Sc)	Design Professional	Private
5	Civil Engineer	Field Engineer	Private
6	Civil Engineer	Occupational Health and Safety Inspector	Private
7	Civil Engineer (M.Sc)	Construction Project Manager	Private
8	Civil Engineer (M.Sc)	Occupational Health and Safety Inspector	Private
9	Civil Engineer	Site Manager (Superintendent)	Private
10	Civil Engineer	Occupational Health and Safety Inspector	Private

Table 10. Participant questions.

No.	Questions
1	Do you consider the obtained site layout plan appropriate? If not, please briefly indicate which facilities' locations may lead to increased on-site risks and explain why.
2	Within the scope of this project, how would you locate the temporary facilities, considering interaction flow, closeness, and tower crane to minimize the potential risks in the construction site? If your proposed layout differs from the optimization-based layout, please briefly explain the reason for this difference.
3	The generation of the optimized layout took approximately 1000 s. Would you prefer an alternative layout that requires around 215 s to compute but yields a slightly higher risk value, with no major differences in the overall site layout? Please explain why.
4	If a user-friendly optimization tool (either a PC or mobile application) were developed for solving facility layout problems, which allows project-specific details and coordinates to be entered, would you consider using it to address site layout problems encountered in practice? Please explain why or why not.

In terms of expert agreement, the qualitative feedback revealed a high level of consistency among the participants. It has emerged that the majority of the experts considered the DA-based layout solution to be more efficient and safer compared to manually generated layouts. Although the participants were asked to locate the facilities by considering predefined parameters, it is seen that some conditions, such as interaction flows, were not adequately accounted for by most participants. While more conventional parameters, such as maintaining a distance between non-hazardous material waste areas and electrical generators, were generally observed, other parameters, such as dust exposure, were frequently overlooked. Furthermore, most participants expressed a clear preference for layouts with lower risk values, even if longer computation times were required. Also, it has been commonly preferred to locate facilities as far as possible from tower cranes, indicating risk

awareness among most participants. This consistency among expert judgments supports the reliability and practical relevance of the proposed optimization-based layout model.

It should also be noted that the expert assessment in this study was designed as a validation of the DA-based layout results. The experts were asked to evaluate and, if necessary, comment on the optimized layouts by considering the same parameters in the DA objective function, which are interaction flow, closeness factor, and tower crane-related risks. As a result, most expert feedback was collected in the form of qualitative assessments and suggested adjustments to the DA-generated optimal layout, rather than generated alternative layouts with defined geometric coordinates. Therefore, the validation was carried out by examining the consistency between expert judgments and the acquired optimization result.

The current state-of-the-art in CSLP mainly involves the customization of existing algorithms for determined project constraints [51–54]. They provide insights into the objective of effective layout plans that aim to maximize optimization with respect to cost and safety objectives [19,93]. In addition, validations of these models are often specific to the cases studied [2,32]. However, construction site risk is still less frequently modeled as a primary optimization objective; furthermore, when included, it is often represented through simplified or problem-specific expressions that may not fully capture the combined effect of interacting hazards [50,94]. The results of this study contribute to the state of the art by (i) defining a risk-driven objective structure that integrates interaction-flow (*RF*), closeness-based risk (*RS*), and crane-related risk (*RC*) within a single formulation, (ii) adapting and implementing the DA as the search mechanism for this risk-focused CSLP, and (iii) demonstrating practical relevance through results compared to the GA and PSO and validation via structured expert feedback. Consequently, this study contributes a risk-based optimization framework for construction site layout planning by integrating OHS-related risk parameters with the DA. The proposed model not only applies the theoretical integration of safety metrics into metaheuristic optimization but also demonstrates practical applicability through a case study.

From a construction safety and management perspective, the effectiveness of the DA-based layout optimization in reducing site risk can be explained by its alignment with particular OHS principles. In construction sites, risk mitigation is essential and many safety incidents arise from repeated exposure to risk sources, such as intersecting material and equipment flows, congested work zones, the location of facilities that constitute risk to each other, and proximity to crane-related operations. The optimized layout rearranges temporary facilities in a manner that reduces these exposures by increasing spatial distance between high-risk incidents derived from interaction flows and conflict-prone zones. In addition, the interaction among different risk parameters plays a critical role in risk mitigation. Interaction flow and closeness-related risks are related, as high traffic intensity combined with facilities that have inadequate distances between them significantly increases the probability of collisions, near-misses, and unsafe worker movements. Crane-related risk, although more specific, represents high-severity hazards that enhance overall site risk when combined with close facility arrangements or heavily intense flow routes. The DA-based optimization reflects safety management strategies because risk reduction is achieved not by focusing on a single risk, but by controlling the effect of multiple interacting risk sources. Consequently, the frequency and intensity of unsafe interactions are mitigated at the planning stage, which is consistent with the approach widely adopted in construction safety management.

7. Conclusions

In our study, risks at construction sites were defined as components of quantitative or qualitative relationships and distances between facilities, because increasing the safety level at a construction site depends on the minimization of the risk factors. Three parameters, which are interaction flow (*RF*), closeness factor (*RS*), and tower crane (*RC*), were considered based on facility relationships to reduce site risk in layout plans. Site risks were modeled based on matrix representation. A DA-based model was developed for the CSLP problem. This model highlights the significance of the study and contributes to CSLP optimization as a means of creating efficient layout plans. To validate the model, a lifestyle resort construction project was used as a case study. PSO and GA algorithms were also applied to the same CSLP problem, and results showed that DA offers better layouts. Also, the results were discussed by participants who had experience locating facilities at construction sites. The feedback demonstrated a high level of consensus among experts, with most participants agreeing on the effectiveness of the proposed layout. In conclusion, feasible layout plans with reduced site risk were obtained as a result of this study. Addressing the gap that site risk is still rarely considered as a primary optimization objective in CSLP, this study proposes a risk-focused approach that accounts for interaction flow (*RF*), closeness-based risk (*RS*), and crane-related risk (*RC*). The case-study results, supported by comparison to GA and PSO and structured expert feedback, indicate that the proposed DA-based framework can generate feasible layouts with reduced site risk and also provide support for OHS-oriented layout decision-making.

As limitations, the DA-based model structure is flexible and can be adapted to various construction contexts with appropriate parameter adjustment, although direct transferability requires careful consideration of site-specific conditions. The definition of site risks can be enhanced, such as laborers' poor psychological conditions and supervision efficiency, which can be determined as a parameter for hazard mitigation. In the DA-based model, a safety-cost trade-off analysis can be conducted to determine the optimal layout plan. Also, due to the nature of the DA, different solutions can be achieved by changing or tuning the coefficients (s, a, c).

It should be noted that the optimization process depends as much on the experience of project managers or decision makers as it does on data collected from the site. In addition, the post-safety situation of the site was not tracked within the scope of this study. Future research can focus on empirical validation through real-site monitoring to quantify the tangible safety improvements achieved by the optimized layout. Moreover, future studies may extend the proposed framework by incorporating construction productivity as an additional objective within a multi-objective optimization. Early CSLP studies mostly focused on the cost parameter in single-objective research and extended to multi-objective studies. For instance, material handling efficiency, travel distances, and operational delays could be considered with safety-related risks. The current single-objective optimization can be extended by adding efficiency-related objectives and solving the problem using a weighted-sum approach or Pareto-based multi-objective metaheuristics. Thus, it would enable the determination of trade-offs between safety and productivity and support more balanced construction site layout decisions. In this study, however, the optimization problem was intentionally formulated as a single-objective model focusing solely on risk minimization to evaluate DA performance as a baseline before considering additional objectives.

While this study treats CSLP as a static optimization problem, real construction projects typically undergo dynamic changes that may require layout adjustments during construction phases. However, the proposed framework is most directly applicable as a decision-support tool for early phases of construction to establish a baseline layout that reduces exposure to risk factors under the defined site constraints. In practice, the same frame-

work can be operated at predefined milestones such as major trade transitions or crane relocations, using updated inputs to generate stage-specific layouts, without changing the model structure. Future research can be extended to a fully dynamic CSLP by incorporating multi-stage decision variables. Additionally, multi-objective trade-offs can be employed by embedding the cost parameter in the optimization framework.

The applicability of the proposed DA-based CSLP optimization framework is primarily associated with site safety, which is strongly influenced by selected risk parameters. The model is particularly suitable for projects with clearly defined site boundaries, temporary facility layouts, and risk mechanisms that can be quantitatively represented. While the framework is adaptable through the administration of risk parameters, its generalization to different construction scales or alternative risk scenarios requires validation. Therefore, this study demonstrates the effectiveness of the proposed approach within its defined problem scope.

It was recognized that the optimization results could be further evaluated within a comprehensive benchmarking framework by considering the best solutions by employing other mainstream bio-inspired algorithms. Also, to demonstrate the generality of the algorithm, repeated experiments, different case studies, and statistical significance tests can be executed. Additionally, the proposed DA-based model can be applied to another case study. However, it was intentionally left outside the scope of the present study to maintain focus on the proposed risk-based CSLP optimization framework; otherwise, it would have resulted in the study becoming overly extended.

Supplementary Materials: The following supporting information can be downloaded at: https://www.mdpi.com/article/10.3390/buildings16050961/s1, Material, equipment, and information flows; risk matrices for closeness factor; optimization results for each population value and iteration count; box plots of optimization results. Figure S1: mean-standard deviation values for 50-population size; Figure S2: mean-standard deviation values for 100-population size; Figure S3: mean-standard deviation values for 200-population size; Table S1: material flow; Table S2: equipment flow; Table S3: information flow; Table S4: the closeness factor between facilities for the non-hazardous material waste (MW) parameter; Table S5: the closeness factor between facilities for the dust (DU) parameter; Table S6: the closeness factor between facilities for the vibration (VI) parameter; Table S7: the closeness factor between facilities for the uncomfortable temperature (UT) parameter; Table S8: the closeness factor between facilities for the explosives and inflammable material (EIM) parameter; Table S9: The closeness factor between facilities for the high electric voltage (EV) parameter; Table S10: The closeness factor between facilities for the hazardous chemicals (CH) parameter; Table S11: Results for 50 population size; Table S12: Results for 100 population size; Table S13: Results for 200 population size.

Author Contributions: Conceptualization, Y.O.T.; methodology, Y.O.T.; software, Y.O.T.; validation, Y.O.T. and S.B.; formal analysis, S.B.; investigation, Y.O.T. and S.B.; resources, S.B.; data curation, Y.O.T. and S.B.; writing—original draft preparation, Y.O.T.; writing—review and editing, S.B.; visualization, Y.O.T.; supervision, S.B.; project administration, Y.O.T. All authors have read and agreed to the published version of the manuscript.

Funding: This research received no external funding.

Institutional Review Board Statement: The study was conducted in accordance with the Declaration of Helsinki and approved by the Institutional Review Board of Ege University (10548779, 2 June 2023).

Informed Consent Statement: Informed consent was obtained from all subjects involved in the study. Participation was voluntary, and no identifiable personal data were collected.

Data Availability Statement: All data generated or used during the study are available from the corresponding author by request.

Acknowledgments: We express our gratitude to Folkart Construction for sharing their construction projects and site data.

Conflicts of Interest: The authors declare no conflicts of interest.

Abbreviations

The following abbreviations are used in this manuscript:

ABC	Artificial Bee Colony Algorithm
ACO	Ant Colony Optimization
AI	Absolutely Important
BLS	Bureau of Labor Statistics
CHs	Chemicals
CSLP	Construction Layout/Site Layout Planning
CSLP	Construction Site Layout Planning
DA	Dragonfly Algorithm
DU	Dust
EF	Equipment Flow
EI	Extremely Important
EIMs	Explosives and Inflammable Materials
EVs	Electrical Voltages
G	Shaft width (crane parameter)
GA	Genetic Algorithm
HS	Hazardous Situations
I	Important
IF	Information Flow
J	Jib length (crane parameter)
LF	Labor Flow
MF	Material Flow
MOPSO	Multi-Objective Particle Swarm Optimization
MW	Material Waste
NI	Not Important
NO	Noise
OHS	Occupational Health and Safety
OSHA	Occupational Safety and Health Administration
PSO	Particle Swarm Optimization
QAP	Quadratic Assignment Problem
RC	Tower Crane Risk
RF	Interaction Flow Risk
RS	Closeness Factor Risk
SLP	Systematic Layout Planning
SSI	Social Security Institution of Turkey
SW	Site Waste
TR	Total Risk
UBC	Uniform Building Code
UI	Unimportant
UT	Uncomfortable Temperature
VI	Very Important
VI	Vibration

References

1. Xu, M.; Mei, Z.; Luo, S.; Tan, Y. Optimization algorithms for construction site layout planning: Review. *Eng. Constr. Archit. Manag.* **2020**, *27*, 1913–1938. [CrossRef]
2. Borges, M.L.A.E.; Granja, A.D.; Monteiro, A. A Hybrid framework for multi-objective construction site layout optimization. *Buildings* **2024**, *14*, 3790. [CrossRef]
3. Adrian, A.M.; Utamima, A.; Wang, K.J. Comparative study of GA, PSO and ACO for solving construction site layout optimization. *KSCE J. Civ. Eng.* **2015**, *19*, 520–527. [CrossRef]
4. Mirjalili, S. Dragonfly algorithm: A new meta-heuristic. *Neural Comput. Appl.* **2016**, *27*, 1053–1073. [CrossRef]
5. Alshinwan, M.; Abualigah, L.; Shehab, M.; Elaziz, M.A.; Khasawneh, A.M.; Alabool, H.; Hamad, H.A. Dragonfly algorithm: A comprehensive survey of its results, variants, and applications. *Multimed. Tools Appl.* **2021**, *80*, 14979–15016. [CrossRef]
6. Pham, H.T.; Dau, H.H.; Nguyen, D.T. Modified dragonfly algorithm for solving the temporary facility location planning problem in construction sites. *KSCE J. Civ. Eng.* **2025**, *29*, 100275. [CrossRef]
7. Rahman, C.M.; Rashid, T.A. Dragonfly algorithm and its applications in applied science survey. *Comput. Intell. Neurosci.* **2019**, *2019*, 9293617. [CrossRef]
8. Meraihi, Y.; Ramdane-Cherif, A.; Acheli, D.; Mahseur, A. Dragonfly algorithm: A comprehensive review. *Neural Comput. Appl.* **2020**, *32*, 16625–16646. [CrossRef]
9. Emambocus, B.A.S.; Jasser, M.B.; Mustapha, A.; Amphawan, A. Dragonfly algorithm and its hybrids: A survey on performance, objectives and applications. *Sensors* **2021**, *21*, 7542. [CrossRef]
10. Razavi, F.K.J.; Mahmood, M.; Wang, D.; AL-Azzawi, O.; AL-Jamely, A. Heuristic dragonfly algorithm for optimal design of truss structures with discrete variables. *Structures* **2021**, *29*, 843–862. [CrossRef]
11. Rahman, C.M.; Rashid, T.A.; Alsadoon, A.; Bacanin, N.; Fattah, P.; Mirjalili, S. Survey on dragonfly algorithm. *Evol. Intell.* **2023**, *16*, 1–21. [CrossRef]
12. Sing, M.C.; Fung, I.W.; Edwards, D.J.; Liu, H. Dynamic construction site layout planning: Branch and bond algorithm. *Int. J. Build. Pathol. Adapt.* **2022**, *40*, 523–538. [CrossRef]
13. Abdelalim, A.M.; Kenawy, A.M.; Aman, K. Construction site layout planning considering travelling distance cost and safety relationships using a genetic algorithm technique. *Int. J. Constr. Eng. Manag. Compet.* **2024**, *14*, 3–20. [CrossRef]
14. Yin, H. Multi-objective optimization of construction management site layout. *Syst. Soft Comput.* **2024**, *6*, 200113. [CrossRef]
15. Ahumada, C.B.; Quddus, N.; Mannan, M.S. A method for facility layout optimisation including stochastic risk assessment. *Process Saf. Environ. Prot.* **2018**, *117*, 616–628. [CrossRef]
16. Salah, M.; Khallaf, R.; Elbeltagi, E.; Wefki, H. Construction site layout planning: A social network analysis. *Buildings* **2023**, *13*, 2637. [CrossRef]
17. Tao, G.; Feng, J.; Feng, H.; Feng, H.; Zhang, K. Reducing construction dust pollution by planning construction site layout. *Buildings* **2022**, *12*, 531. [CrossRef]
18. Yao, Z.; Chen, Z.; Lee, Y. A construction site layout planning study for dust reduction. *J. Constr. Eng. Manag.* **2025**, *151*, 04025066. [CrossRef]
19. Wefki, H.; Salah, M.; Elbeltagi, E.; Elsheikh, A.; Khallaf, R. A generative design-based optimization model for multi-objective construction site layout planning. *Eng. Constr. Archit. Manag.* **2025**, *32*, 5429–5455. [CrossRef]
20. Social Security Institution of Turkey (SSI). Annual of Statistics 2020. Available online: http://www.sgk.gov.tr/ (accessed on 27 June 2021).
21. Bureau of Labor Statistics (BLS). Occupational Injuries and Illnesses and Fatal Injuries Profiles. 2020. Available online: https://data.bls.gov/gqt/ProfileData (accessed on 27 June 2021).
22. El-Rayes, K.; Khalafallah, A. Trade-off between safety and cost in planning construction site layouts. *J. Constr. Eng. Manag.* **2005**, *131*, 1186–1195. [CrossRef]
23. Medina-Herrera, N.; Jiménez-Gutiérrez, A.; Grossmann, I.E. Optimal layout considering quantitative risk. *Comput. Chem. Eng.* **2014**, *69*, 165–181. [CrossRef]
24. Rezaee, M.; Shakeri, E.; Ardeshir, A.; Malekitabar, H. Optimizing travel distance of construction workers considering their behavioral uncertainty using fuzzy graph theory. *Autom. Constr.* **2021**, *124*, 103574. [CrossRef]
25. Abune'meh, M.; El Meouche, R.; Hijaze, I.; Mebarki, A.; Shahrour, I. Optimal construction site layout based on risk spatial variability. *Autom. Constr.* **2016**, *70*, 167–177. [CrossRef]
26. El-Meouche, R.; Abunemeh, M.; Hijaze, I.; Mebarki, A. Developing optimal paths for evacuating risky construction sites. *J. Constr. Eng. Manag.* **2017**, *144*, 04017098. [CrossRef]
27. Ning, X.; Qi, J.; Wu, C. quantitative safety risk assessment model for site layout planning. *Saf. Sci.* **2018**, *104*, 246–259. [CrossRef]
28. Zavari, M.; Shahhosseini, V.; Ardeshir, A.; Sebt, M.H. Multi-objective dynamic construction site layout using BIM and GIS. *J. Build. Eng.* **2022**, *52*, 104518. [CrossRef]

29. Soliman, A.A.; Mohammed, A.A.; Ibrahim, A.H. Dynamic site layout optimization using DRL with PPO. *Eng. Constr. Archit. Manag.* **2025**, 1–25. [CrossRef]
30. Tate, D.M.; Smith, A.E. Unequal-area facility layout by genetic search. *IIE Trans.* **1995**, *27*, 465–472. [CrossRef]
31. Salah, M.; Elbeltagi, E.; Elsheikh, A. Optimization of construction site layout using BIM generative design. *Int. J. Constr. Manag.* **2024**, *24*, 314–322. [CrossRef]
32. Albayrak, G. Solving construction site layout planning as a quadratic assignment problem using the advanced jaya algorithm. *Appl. Sci.* **2025**, *15*, 10295. [CrossRef]
33. Yeh, I.C. Construction-Site Layout Using Annealed Neural Network. *J. Comput. Civ. Eng.* **1995**, *9*, 201–208. [CrossRef]
34. Karray, F.; Zaneldin, E.; Hegazy, T.; Shabeeb, A.H.M.; Elbeltagi, E. Tools of soft computing as applied to facilities layout. *IEEE Trans. Fuzzy Syst.* **2000**, *8*, 367–379. [CrossRef]
35. Kaveh, A.; Khanzadi, M.; Alipour, M.; Moghaddam, M.R. Construction site layout planning using two new meta-heuristic algorithms. *Iran. J. Sci. Technol. Civ. Eng.* **2016**, *40*, 263–275. [CrossRef]
36. Kaisar, K.; Farmakis, P.; Tsikas, P.; Chassiakos, A.P. Evolutionary algorithms for construction site layout planning. In *Creative Construction Conference 2023*; Budapest University of Technology and Economics: Budapest, Romania, 2023. [CrossRef]
37. Tao, G.; Feng, H.; Feng, J.; Wang, T. Dynamic multi-objective construction site layout based on BIM. *KSCE J. Civ. Eng.* **2022**, *26*, 1522–1534. [CrossRef]
38. Pham, V.H.S.; Pham, D.H. Dynamic Multiobjective optimization model for construction site layout in prefabricated projects. *J. Constr. Eng. Manag.* **2025**, *151*, 04025150. [CrossRef]
39. Mawdesley, M.J.; Al-Jibouri, S.H. Proposed genetic algorithms for construction site layout. *Eng. Appl. Artif. Intell.* **2003**, *16*, 501–509. [CrossRef]
40. Xu, J.; Zhao, S.; Li, Z.; Zeng, Z. Bi-Level construction site layout optimization based on hazardous material transportation. *J. Infrastruct. Syst.* **2016**, *22*, 04016014. [CrossRef]
41. Zhang, H.; Wang, J.Y. Particle swarm optimization for construction site unequal-area layout. *J. Constr. Eng. Manag.* **2008**, *134*, 739–748. [CrossRef]
42. Benjaoran, V.; Peansupap, V. Grid-based construction site layout planning with particle swarm optimisation and travel path distance. *Constr. Manag. Econ.* **2019**, *38*, 673–688. [CrossRef]
43. Lam, K.; Ning, X.; Ng, T. Application of ant colony optimization to site layout planning. *Constr. Manag. Econ.* **2007**, *25*, 359–374. [CrossRef]
44. Zouein, P.P.; Kattan, S. Ant colony optimization for dynamic facility layout. *J. Oper. Res. Soc.* **2021**, *73*, 1517–1531. [CrossRef]
45. Yahya, M.; Saka, M.P. Site layout using multi-objective artificial bee colony algorithm. *Autom. Constr.* **2014**, *38*, 14–29. [CrossRef]
46. Liang, L.Y. Improved cost optimization algorithm for site building layout planning. *Archit. Sci. Rev.* **2008**, *51*, 269–276. [CrossRef]
47. Jaafar, K.; Elbarkouky, R.; Kennedy, J. Construction site layout optimization model considering cost and safety in a dynamic environment. *Asian J. Civ. Eng.* **2021**, *22*, 297–312. [CrossRef]
48. Gad, H.K.; Ali, M.H.; Eldesouky, A.; Abdullatif, A.; Serry, M.; Ossama, H.; Essawy, Y.A. Irregular dynamic site layout optimization model. In *Proceedings of CSCE 2022*; Springer: Cham, Switzerland, 2023; pp. 391–402.
49. Li, X.; Zhang, Z.; Ma, Y.; Yao, Y.; Hao, Y.; Chai, R. Construction site layout optimization algorithm based on MOPSO. In *Proceedings of the 2023 China Automation Congress (CAC), Chongqing, China, 7–19 November 2023*; IEEE: New York, NY, USA, 2023; pp. 3405–3410. [CrossRef]
50. Nguyen, P.T. Construction site layout planning and safety management using a fuzzy bee colony model. *Neural Comput. Appl.* **2021**, *33*, 5821–5842. [CrossRef]
51. Proyogo, D.; Sutanto, J.C.; Suryo, H.E.; Eric, S. Comparative study on bio-inspired algorithms in construction layout. *Civ. Eng. Dimens.* **2018**, *20*, 102–110. [CrossRef]
52. Kaveh, A.; Moghaddam, M.R.; Khanzadi, M. Efficient Multi-objective optimization algorithms for construction site layout. *Iran. J. Sci. Technol. Civ. Eng.* **2018**, *25*, 2051–2062. [CrossRef]
53. Al Hawarneh, A.; Bendak, S.; Ghanim, F. Construction site layout planning problem: Past, present and future. *Expert Syst. Appl.* **2021**, *168*, 114247. [CrossRef]
54. Tsegay, F.G.; Mwanaumo, E.; Mwiya, B. Mathematical optimization for inner-city site layout: Systematic review. *Asian J. Civ. Eng.* **2023**, *24*, 3781–3795. [CrossRef]
55. Spišáková, M.; Mandičák, T. Construction safety risks management and construction site. In *International Conference Current Issues of Civil and Environmental Engineering Lviv-Košice–Rzeszów*; Blikharskyy, Z., Koszelnik, P., Lichołai, L., Nazarko, P., Katunský, D., Eds.; Lecture Notes in Civil Engineering; Springer: Cham, Switzerland, 2024; Volume 438. [CrossRef]
56. Razavi Alavi, S.; Abou Rizk, S. Construction site layout planning using a simulation-based decision support tool. *Logistics* **2024**, *5*, 65. [CrossRef]
57. Elbeltagi, E.; Hegazy, T.; Eldosouky, A. Dynamic layout of construction temporary facilities considering safety. *J. Constr. Eng. Manag.* **2004**, *130*, 534–541. [CrossRef]

58. Xu, J.; Li, Z. Multi-objective dynamic construction site layout planning in fuzzy random environment. *Autom. Constr.* **2012**, *27*, 155–169. [CrossRef]
59. Abunemeh, M. Construction Site Layout Optimization, Considering Risk of Natural or Technological Hazard Utilizing GIS. 2017. Available online: https://tel.archives-ouvertes.fr/tel-01631400 (accessed on 1 November 2025).
60. Hegazy, T.; Elbeltagi, E. EvoSite: Evolution-based model for site layout planning. *J. Comput. Civ. Eng.* **1999**, *13*, 198–206. [CrossRef]
61. Papadaki, I.N.; Chassiakos, A.P. Multi-objective site layout using genetic algorithms. *Procedia Eng.* **2016**, *164*, 20–27. [CrossRef]
62. Li, Z.; Shen, W.; Xu, J. Bilevel and multi-objective dynamic construction site layout and security planning. *Autom. Constr.* **2015**, *57*, 1–16. [CrossRef]
63. Hammad, A.W.A. A Multi-Objective construction site layout planning problem solved through integration of location and traffic assignment model. *Constr. Manag. Econ.* **2019**, *38*, 756–772. [CrossRef]
64. Taghaddos, H.; Heydari, M.H.; Asgari, A. A hybrid simulation approach for site layout planning in construction projects. *Constr. Innov. Inf. Process Manag.* **2021**, *21*, 417–440. [CrossRef]
65. Hou, S.; Wen, H.; Feng, S.; Wang, H.; Li, Z. Application of layered coding genetic algorithm in optimization of unequal area production facilities layout. *Comput. Intell. Neurosci.* **2019**, *2019*, 3650923. [CrossRef]
66. Zuo, J.; Rameezdeen, R.; Hagger, M.; Zhou, Z.; Ding, Z. Dust pollution control on construction sites. *J. Clean. Prod.* **2017**, *166*, 312–320. [CrossRef]
67. Ning, X.; Qi, J.; Wu, C.; Wang, W. Reducing noise pollution via site layout optimization. *J. Clean. Prod.* **2019**, *222*, 218–230. [CrossRef]
68. Zhang, X.; Zhang, W.; Jiang, L.; Zhao, T. Identification of critical causes of tower-crane accidents through system thinking and case analysis. *J. Constr. Eng. Manag.* **2020**, *146*, 04020071. [CrossRef]
69. Sadeghi, S.; Soltanmohammadlou, N.; Rahnamayiezekavat, P. Systematic review of crane safety requirements. *Saf. Sci.* **2021**, *133*, 105002. [CrossRef]
70. Huang, C.; Wang, Z.K.; Li, B.; Wang, C.; Xu, L.S.; Jiang, K.; Liu, M.; Guo, C.X.; Zhao, X.F.; Yang, H. Discretized cell modeling for optimal layout of multiple tower cranes. *J. Constr. Eng. Manag.* **2023**, *149*, 04023068. [CrossRef]
71. Oral, M.; Bazaati, S.; Aydinli, S.; Oral, E. Construction site layout planning via multi-objective PSO. *Tek. Dergi* **2018**, *29*, 8691–8713. [CrossRef]
72. Sanad, H.M.; Ammar, M.A.; Ibrahim, M.E. Optimal site layout considering safety & environment. *J. Constr. Eng. Manag.* **2008**, *134*, 536–544. [CrossRef]
73. Muther, R. *Systematic Layout Planning*; CBI Publishing: Boston, MA, USA, 1973.
74. Kim, K.J.; Kim, K. Case study on the evaluation of equipment flow at a construction site. *J. Comput. Civ. Eng.* **2010**, *24*, 570–575. [CrossRef]
75. Dweiri, F.; Meier, F.A. Application of fuzzy decision-making in facilities layout planning. *Int. J. Prod. Res.* **1996**, *34*, 3207–3225. [CrossRef]
76. Ning, X.; Lam, K.-C.; Lam, M.-C. Dynamic construction site layout planning using max–min ant system. *Autom. Constr.* **2010**, *19*, 55–65. [CrossRef]
77. Liu, Y.N.; Zhao, Q.L. *Proceedings of China Modern Logistics Engineering: Research on Logistic Center Layout Based on SLP*; Springer: Berlin/Heidelberg, Germany, 2015; Volume 286, pp. 17–28.
78. Kines, P.; Andersen, L.P.S.; Spangenberg, S.; Mikkelsen, K.L.; Dyreborg, J.; Zohar, D. Improving construction site safety through leader-based verbal communication. *J. Saf. Res.* **2010**, *41*, 399–406. [CrossRef]
79. Yang, X.-S. Firefly algorithm and global optimization. In *Research and Development in Intelligent Systems XXVI*; Springer: London, UK, 2010; pp. 209–218.
80. Osman, H.M.; Georgy, M.E.; Ibrahim, M.E. Hybrid CAD-based site layout planning using GAs. *Autom. Constr.* **2003**, *12*, 749–764. [CrossRef]
81. Kaya, S.; Fığlalı, N. Çok amaçlı optimizasyon problemlerinde pareto optimal kullanımı. *Soc. Sci. Res. J.* **2016**, *5*, 9–18.
82. Ning, X.; Qi, J.; Wu, C.; Wang, W. A Tri-objective ant colony optimization model. *Autom. Constr.* **2018**, *89*, 1–12. [CrossRef]
83. Kim, M.; Ryu, H.-G.; Kim, T.W. A typology model of TFL constraints for automated site layout planning. *Appl. Sci.* **2021**, *11*, 1027. [CrossRef]
84. OSHA. Occupational Safety and Health Administrations. In *Construction Industry*; USDOL: Washington, DC, USA, 1987; pp. 19–26.
85. Aranha, C.; Villalón, C.L.C.; Campelo, F.; Dorigo, M.; Ruiz, R.; Sevaux, M.; Sörensen, K. Metaphor-based metaheuristics: A call for action. *Swarm Intell.* **2022**, *16*, 1–6. [CrossRef]
86. Jafari-Asl, J.; Azizyan, G.; Monfared, S.A.H.; Rashki, M.; Andrade-Campo, A.G. Enhanced binary dragonfly algorithm for optimization of pump scheduling. *Eng. Fail. Anal.* **2021**, *123*, 105323. [CrossRef]
87. Tian, H.; Yuan, C.; Li, K. Robust optimization based on multi-objective dragonfly algorithm. *Eng. Appl. Artif. Intell.* **2021**, *106*, 104448. [CrossRef]

88. Indramaya, E.; Suyanto, S. Comparative study of recent swarm algorithms for continuous optimization. *Procedia Comput. Sci.* **2021**, *179*, 685–695. [CrossRef]
89. Joshi, M.; Kalita, K.; Jangir, P.; Ahmadianfar, I.; Chakraborty, S. Conceptual comparison of dragonfly algorithm variants for CEC-2021 problems. *Arab. J. Sci. Eng.* **2023**, *48*, 1563–1593. [CrossRef]
90. *Uniform Building Code (UBC)*; International Conference of Building Officials: Whittier, CA, USA, 1985; pp. 658–660.
91. OSHA. *Safety and Health Regulations for Construction*; 29 CFR Part 1926; API (American Petroleum Institute): Washington, DC, USA, 2003.
92. Khalafallah, A.M. Assessing the performance of the non-dominated sorting genetic algorithm in optimizing construction site planning. *Comput. Civ. Build. Eng.* **2014**, *8*, 1254–1261. [CrossRef]
93. Pham, V.H.S.; Pham, D.H.; Nguyen, T.A. Optimizing construction site layouts with dynamic multi-objective methods and time-based facility placement. *Eng. Constr. Archit. Manag.* **2025**, 1–29. [CrossRef]
94. Javaherikhah, A.; Alimohammadi, P.; Sarvari, H.; Edwards, D.J.; Chan, D.W.M.; Cheung, C. Factors influencing the safety enhancement and cost reduction in site layouts of construction projects. *Buildings* **2025**, *15*, 1089. [CrossRef]

Disclaimer/Publisher's Note: The statements, opinions and data contained in all publications are solely those of the individual author(s) and contributor(s) and not of MDPI and/or the editor(s). MDPI and/or the editor(s) disclaim responsibility for any injury to people or property resulting from any ideas, methods, instructions or products referred to in the content.